sustainability

MDPI

Review

Functionalized Carbon Nanotubes (CNTs) for Water and Wastewater Treatment: Preparation to Application

Mian Muhammad-Ahson Aslam [1], Hsion-Wen Kuo [1,*], Walter Den [2,*], Muhammad Usman [3], Muhammad Sultan [4,*] and Hadeed Ashraf [4]

[1] Department of Environmental Science and Engineering, Tunghai University, No. 1727, Section 4, Taiwan Boulevard, Xitun District, Taichung City 407, Taiwan; ahson17@gmail.com
[2] Department of Science and Mathematics, Texas A&M University—San Antonio, One University Way, San Antonio, TX 78224, USA
[3] Institute for Water Resources and Water Supply, Hamburg University of Technology, Am Schwarzenberg—Campus 3, 20173 Hamburg, Germany; muhammad.usman@tuhh.de
[4] Department of Agricultural Engineering, Bahauddin Zakariya University, Multan 60800, Pakistan; hadeedashraf15@gmail.com
* Correspondence: hwkuo@thu.edu.tw (H.-W.K.); walter.den@tamusa.edu (W.D.); muhammadsultan@bzu.edu.pk (M.S.); Tel.: +886-(4)2359-0121 (ext. 3363) (H.-W.K.); +1-(210)784-2815 (W.D.); +92-333-610-8888 (M.S.)

check for updates

Citation: Aslam, M.M.-A.; Kuo, H.-W.; Den, W.; Usman, M.; Sultan, M.; Ashraf, H. Functionalized Carbon Nanotubes (CNTs) for Water and Wastewater Treatment: Preparation to Application. *Sustainability* **2021**, *13*, 5717. https://doi.org/10.3390/su13105717

Academic Editors: Muhammad Sultan, Yuguang Zhou, Redmond R. Shamshiri and Aitazaz A. Farooque

Received: 24 April 2021
Accepted: 10 May 2021
Published: 19 May 2021

Publisher's Note: MDPI stays neutral with regard to jurisdictional claims in published maps and institutional affiliations.

Copyright: © 2021 by the authors. Licensee MDPI, Basel, Switzerland. This article is an open access article distributed under the terms and conditions of the Creative Commons Attribution (CC BY) license (https://creativecommons.org/licenses/by/4.0/).

Abstract: As the world human population and industrialization keep growing, the water availability issue has forced scientists, engineers, and legislators of water supply industries to better manage water resources. Pollutant removals from wastewaters are crucial to ensure qualities of available water resources (including natural water bodies or reclaimed waters). Diverse techniques have been developed to deal with water quality concerns. Carbon based nanomaterials, especially carbon nanotubes (CNTs) with their high specific surface area and associated adsorption sites, have drawn a special focus in environmental applications, especially water and wastewater treatment. This critical review summarizes recent developments and adsorption behaviors of CNTs used to remove organics or heavy metal ions from contaminated waters via adsorption and inactivation of biological species associated with CNTs. Foci include CNTs synthesis, purification, and surface modifications or functionalization, followed by their characterization methods and the effect of water chemistry on adsorption capacities and removal mechanisms. Functionalized CNTs have been proven to be promising nanomaterials for the decontamination of waters due to their high adsorption capacity. However, most of the functional CNT applications are limited to lab-scale experiments only. Feasibility of their large-scale/industrial applications with cost-effective ways of synthesis and assessments of their toxicity with better simulating adsorption mechanisms still need to be studied.

Keywords: carbon nanotubes; surface modification; heavy metals; adsorption; water and wastewater treatment

1. Introduction

Rapid urbanization and industrialization has significantly increased the clean water demands in the domestic, industrial, and agricultural sectors [1–3]. Meanwhile, large quantities of pollutants including organic, inorganic, and biological contaminants are being released into the water bodies from these sectors [4–6]. Eccentric waters such as brackish, storm, and wastewater are being used depending upon the purposes [7,8]. Increasingly, use of these waters has also increased the urgent concern about the burden of negative impacts on the surrounding environment; one of the tremendous challenges confronting mankind is the exploration of green and sustainable methods to overcome these shortcomings [9–13]. Keeping in mind the current situation of water and wastewater treatment status, the technologies are not sustainable to meet healthy requirements for surrounding environment and community health [14,15].

Historically, numerous techniques and methods have been investigated for advanced treatment of water and wastewater [16]. The most common, adsorption, was proven to be the improved technique to remove a variety of pollutants including organic and inorganic contaminants present in water and wastewater [17,18]. Limited treatment efficiency was reported by using conventional adsorbents due their small surface area, limited number of active sites, deficiency in selectivity, and low adsorption kinetics [19]. These shortcomings of conventional adsorbents have been addressed in recent advancements of nano-adsorbents owing to their high surface area coupled with a higher number of active sites, tunable pore size, fast kinetics, and improved surface chemistry [10,20–24].

The nanomaterials can be used for treatment of water and desalination as well and also reveal properties including electron affinity, mechanical strength, and flexibility during functionalization [25–27]. Carbon nanomaterials (CNs) such as carbon nanotubes (CNTs) are supposed to be a promising material to break down the tradeoff concerning selectivity and adsorption, resulting in an increase of the economics of adsorption technology [25]. As a result, CNTs, as an adsorbent for treatment of water, have attained the focus of countless scholars over the previous few decades who are projected to carry on the exploration and developments in the field of CNs [28].

Numerous significant articles have been published on nanomaterials applied for the treatment of water and wastewater in previous few years [29–37]. Despite rapid developments, innovations, and applications of CNT-based nanomaterials, there is an increasing need for an across-the-board review of the synthesis of CNTs, functionalization of surface modifications, and finally their application to remove aqueous contaminants and to identify potential directions. This is the main motivation of the current review article.

This review attempts to address a brief history of CNTs, synthesis, purification, and functionalization, followed by the application of these nanomaterials for eliminating organics, inorganics, and microorganisms present in water and wastewater samples.

1.1. Historical Background

The discovery of CNTs was reviewed in 2006 by Monthioux and Kuznetsov, showing that the science has seemed to remain controversial [38]. Most literature mentions that nanotubes were discovered by Sumio Iijima [38]. However, Radushkevich and Lukyanovich explained the synthesis process of CNTs with 50 nm diameter [39]. Oberlin et al. explained the vapor phase growth technique for the synthesis of carbon fibers; the synthesized tubes consisted of turbostratic stacks of carbon layers (i.e., describing a crystal structure in which basal planes have slipped out of alignment) [40]. In addition, Abrahamson et al. [41] described the arc discharge method for carbon fiber synthesis using carbon anodes. Later on, scientists described the thermal catalytic disproportionation of CO for the synthesis of CNs. Transmission electron microscopy (TEM) and X-ray diffraction pattern (XRD) were used to characterize the synthesized CNs, and as a result they believed that CNTs can be formed by a graphene layer turning into a tubular shape. They also concluded that two types of promising arrangements, such as a helix-shaped spiral and circular arrangements in the form of a graphene hexagonal network, can result by turning the graphene layer into a tabular shape [42]. Later, a US patent was issued in 1987 on carbon nanofibers synthesis, the diameter ranging from 3.5 to 70 nm and five times greater in length than the diameter [43].

Back to the dates in 1950s, after the disclosure of CNTs by Iijima, projection of surprising properties of single-walled carbon nanotubes (SWCNTs) made by Dunlap and colleagues also attracted the attention of researchers around the world. At this time, after the discoveries and exploration of SWCNTs by Bethune and Iijima independently at IBM (Shiba, Minato) and Nippon Electric Co., Ltd. (Tokyo, Japan), respectively, the research on CNs and their specific methods of production was extended [44,45].

The above findings seem to be the extension of Fullerence's discovery. Arc discharge technology had previously been applied for the production of laboratory-scale Buckminster

fullerenes [46,47]. CNTs are being studied after the report published in 1991 by Iijima [45] was fundamental, because it put CNTs in the limelight [38].

1.2. Types of CNTs and Structure

CNTs are composed of carbon atoms organized in a progression of fused benzene rings, which are pleated into a cylindrical shape. This new sort of man-made nano-material has a place with fullerene family and is treated as carbon's third allotrope as well as sp^2 and sp^3 forms of graphite and diamond, respectively [42,48,49].

Generally, there are two types of CNTs [50] on the bases of number of layers shown in Figure 1:

1. Single-walled carbon nanotubes (SWCNTs)
2. Multi-walled carbon nanotubes (MWCNTs).

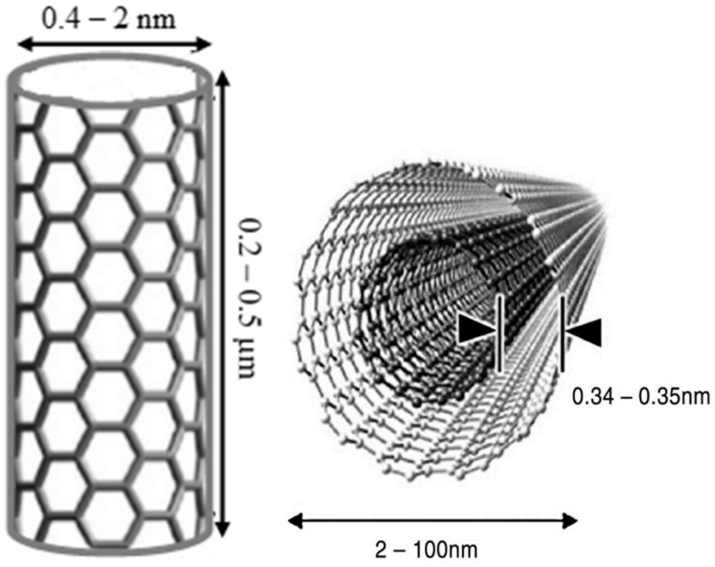

Figure 1. Types of typical dimensions of CNTs, SWCNTs (**left**) and MWCNTs (**right**).

CNTs are made by a sheet of graphene when rolled into a cylindrical shape, which may have a capped or open end, usually in a hexagonal form close packed with a diameter at a small scale of 1 nm, and a few microns long. SWCNTs (Figure 1) with a diameter as small as 0.4 to 2 nm are made by the single sheet of graphene rolled into a cylindrical shape, while MWCNTs (Figure 1) with an outer and inner diameter ranging from 2–100 nm and 1–3 nm, respectively, and a several microns in length are made up of two or more sheets of graphene incasing a hollow core in the same way as in SWCNTs [49,51,52].

Based on the chemistry, there are two zones of CNTs: the sidewall and tip. A significant aspect in controlling these distinctive properties emanates after the change in the tube-like structure due to entrapment of graphene layers into a cylindrical shape. Figure 2 shows different structures of rolled SWCNTs based on graphene sheets. Depending on alignment of the cylinder axis relative to the hexagonal matrix, the CNTs structure can be stipulated by chiral carrier in three ways, armchair, chiral, and zigzag, illustrated by their chirality index (n,m). Geometric arrangement of carbon atoms present at the layer of nanotubes is responsible for the foundation of zigzag (m = 0) and armchair (n = m) CNTs, whereas the structure of the nanotube with the two enantiomorphs on the right side is chiral ($n \neq m$) [53,54].

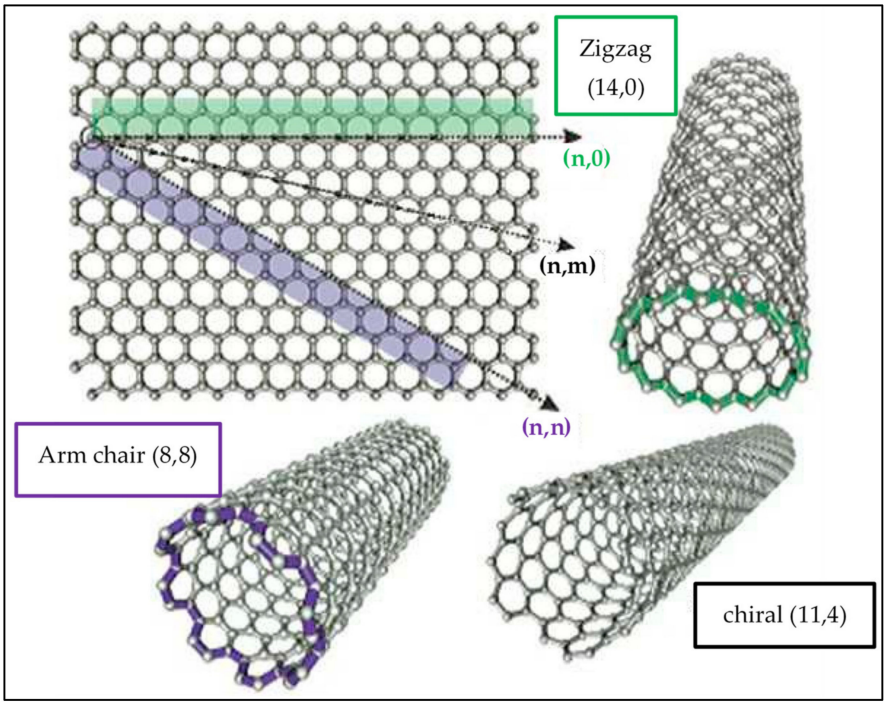

Figure 2. Roll-up of graphene sheet into different types of CNTs [54,55].

Recent reviews are good to find detailed elucidations of the structure of CNTs [48,49,56–61]. Here, Table 1 summarizes a comparison of the properties of SWCNTs and MWCNTs.

Table 1. Comparison between properties of SWCNTs and MWCNTs [49,62,63].

Properties	SWNTs	MWCNTs
Layer type	Single graphene layer	Multiple graphene layer
Catalyst requirement	Essential during synthesis	No need during synthesis
Bulk or massive production	Difficult	Easy
Purity level	Low	Large
Defect's level	High	Low
Characterization	Easy	Difficult
Manage	Easily twisted	Cannot be twisted easily
Specific gravity	About 0.8 g/cm^3	Less than 1.8 g/cm^3
Elastic modulus	About 1.4 TPa	Ranging from 0.3 to 1 TPa
Strength	Ranging from 50 to 500 GPa	Ranging from 10 to 60 GPa
Electrical conductivity	Ranging from 102 to 106 S/cm	Ranging from 103 to 105 S/cm
Electron mobility	About 105 $cm^2/(V\ s)$	Ranging from 104 to 105 $cm^2/(V\ s)$
Thermal conductivity	About 6000 W/(m K)	About 2000 W/(m K)
Coefficient of thermal expansion	Greater than $1.1 \times 10^{-3}\ K^{-1}$	About $-1.37 \times 10^{-3}\ K^{-1}$
Thermal stability in air	Ranging from 600 to 800 °C	Ranging from 600 to 800 °C
Resistivity	Ranging from 50 to 500 μΩ cm	Ranging from 50 to 500 μΩ cm
Specific Surface Area	Ranging from 400 to 900 m^2/g	Ranging from 200 to 400 m^2/g

2. Synthesis of CNTs

Typically, there are three extensive methods for the synthesis of CNTs as given bellow:

(a) Arc discharge
(b) Laser ablation
(c) Chemical vapor deposition (CVD).

CNTs are produced by using energy and carbon sources in all the synthesis methods. A carbon electrode or a gas and an electric current or heat is used as a carbon and energy source, while using arc discharge or CVD methods, respectively, for the synthesis of CNTs,

whereas a laser beam is used as an energy source during the laser ablation method. Table 2 presents a detailed summary of the efficiencies of the CNT synthesis methods. These methods are based on the formation of a single or a consortium of carbon atoms that sack to recombine into CNTs.

CNT synthesis mechanisms have been debated in detail by Cassell et al. [64] and Sinnott et al. [65]. It is believed that by using the metallic catalyst in the CVD method for CNT synthesis, the cylindrical shaped graphene tube is formed by initial deposition of carbon atoms on the used catalyst surface [66]. It was also concluded that the size of particles of the used catalyst also play an important role in the CNTs diameter, as the catalyst particles in a smaller size produce SWCNTs with a diameter of a few nanometers, while the larger particles tend to produce MWCNTs [67].

The arc discharge method between graphite electrodes is the first method of producing CNTs [68]. Briefly, in this method, direct current of 50 to 100 A and about 20 volts of potential difference is established between a graphite electrode pair in the presence of one of the inert gases containing helium or argon with a pressure of 500 Torr [69,70]. The carbon electrode surface evaporates and forms a cylindrical-shaped tube structure because of the high temperature generated due to the discharge of electric current in low pressure, inert gas, and catalyst [44,70,71]. MWCNTs can be synthesized via an arc discharge method without a metallic catalyst; on the other hand, mixed-metal catalysts, for example iron, cobalt, and nickel, are necessary for SWCNTs fabrication [72]. In general, higher levels of structural precision are noted in CNTs produced via the arc discharge method [73]; however, different variables such as chamber temperature, concentration and type of catalyst, hydrogen presence, etc., may affect the structure and size of synthesized CNTs [74]. Recently, nickel-filled CNTs were synthesized via a local arc discharge method in liquid ethanol [75], nitrogen-doped CNTs via vaporization of boron nitride [76], low-cost SWCNTs via an arc discharge method in open air [77], and SWCNTs and MWCNTs via a hot plasma arc discharge method [78].

The use of laser ablation to synthesize CNTs was first reported by Guo and colleagues in 1995 [79,80]. Briefly, a graphite object is targeted by a laser beam with high energy in the presence of argon at 800–1200 °C temperature and 500 Torr pressure [69,70,81,82]. In this method, a laser pulse provides an energy source, and a graphite object serves as a source of carbon. Soot deposition of carbon can be avoided by uniform evaporation of the target resulting because of continuous applications of laser pulses. The larger size particles after the first laser beam are broken down into smaller ones by the successive beams. Later, the smaller size particles are produced into the CNT structure. Commonly, transition metals are used as catalysts in this method. Rope-shaped CNTs can be found by using a laser ablation method with the diameter ranging from 10 to 20 nm and about 100 mm long [83].

CVD is a well-liked method for bulk fabrication of CNTs around the globe. Typically, in this method, carbon monoxide or hydrocarbons gases are used as a source of carbon, while 500 to 1100 °C of temperature is used as the source of energy. The carbon atoms are deposited by the decomposition of the used carbon source and shaped into CNTs [84,85]. Briefly, the decomposition of gas (carbon source) occurs because of high temperature when transferred into reaction chamber together with the carrier gas and generates a substrate of carbon atoms on the surface of catalyst to form CNTs [86]. When compared to other methods of synthesis of CNTs, the CVD is the most common route for relatively large-scale production of CNTs as it is simple in operation, higher in yield, and economic and has a high rate of deposition and good control over the morphology of tubes during the synthesis process [87–89] Cassell et al. [64] studied that CNTs in bulk can be produced, especially SWCNTs via the CVD method, by using acetylene as a source of carbon deposition in the presence of iron and cobalt and zeolite or silica as a carrier support material. They also concluded that SWCNTs can be produced on a largescale when a mixture of H_2 and CH_4 is deposited on the catalyst (Co or Ni), and MgO as carrier support material is used.

Table 2. A summary of CNTs synthesis strategies and their efficiencies.

Parameters		Arc Discharge Method	Chemical Vapor Deposition	Laser Ablation (Vaporization)	Ref.
Method	Source of energy	Direct current	Temperature (ignition)	High intensity laser beam	[90,91]
	Source of carbon	Carbon or graphite electrodes	Hydrocarbon gases or carbon monoxide (CH_4, CO, or acetylene)	Graphite object	
Temperature (°C)		3000 to 4000	500 to 1100	About 3000	[84,85]
Cost per unit synthesis		Costly	Economic	Costly	[83,92]
CNTs selectivity		Less	High	Less	[93]
Availability of carbon source		Complex	Easy	Difficult	[94]
Purification level		More	Less	More	[95]
Nature of synthesis process		Batch	Continuous	Batch	[64,96]
Control on synthesis parameters		Difficult	Easy	Difficult	[97,98]
Energy requirement		High	Low	High	[99]
Design of reactor		Hard	Simple and easy	Hard	[100]
Nanotube graphitization		High	Moderate	High	[101–103]
Typical yield		30 to 90%	20 to 100%	Up to 70%	[84,91,95,104–106]
Typical Diameter	SWCNTs	0.6 to 1.4 nm	0.6 to 4 nm	1 to 2 nm	[87,91,107,108]
	MWCNTs	Inner: 1 to 3 nm Outer: ~10 nm	0.1 to several nanometers	10 to 20 nm	[79,83,91,104,109]

Table 2. *Cont.*

Parameters	Arc Discharge Method	Chemical Vapor Deposition	Laser Ablation (Vaporization)	Ref.
Advantages	1. Synthesis of both SWCNTs and MWCNTs is easy 2. MWCNTs can be produced without any catalyst 3. Costly process but less than laser ablation method 4. Synthesis of CNTs is possible in open air 5. High degree of structural perfection	1. Bulk production is easy 2. More extensive length CNTs than other methods 3. Simple and easy process 4. Quite pure 5. Alignment of produced CNTs is good 6. Diameter and number of layers can be controlled	1. Primarily for SWCNTs 2. Diameter of CNTs can be controlled 3. Lower numbers of defects 4. High degree of structural perfection 5. Tubes' length can vary from 5 to 20 mm	[98,110–113]
Disadvantages	1. Received with some structural defects 2. Short and randomly distributed in length and direction 3. Lot of structural purification is needed 4. Contains carbon impurities	1. Only used to produce MWCNTs 2. Higher structural defect density	1. Costly technique due to expensive lasers beams 3. Power needs are high 4. Low yield	[65,86,98,109]
Figures	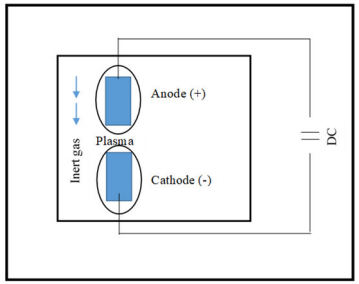	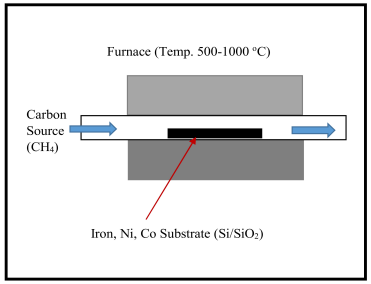	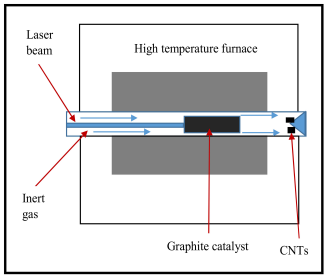	[114]

3. CNT Purifications

Some of the impurities include an amorphous phase of carbon, particles of particular metals, or any other carrier material associated with CNTs that will have an effect on their execution performance [115]. Some typical purification technologies and their characteristics are discussed in Table 3. On average, the CNTs synthesized via the CVD method showed a purity level ranging from 5% to 10% [116]. Therefore, a broad purification of CNTs is necessary before being used for different applications. The detection and identification of different impurities associated with CNTs using different techniques have been discussed in Table 4. It is believed that the CNT structure may be affected to some extent when removing impurities, so there is always need for a compromise with the final structure after purification process [116]. The common CNTs purification methods are discussed below:

1. Oxidation
2. Acid treatment
3. Surfactant based sonication.

Oxidation is a decent manner to remove carbon [117–122] and metal [117,121,123–126] impurities associated with CNTs. One of the main shortcomings that occur using this process of purification is the oxidation of CNTs themselves along with the impurities, but fortunately, the loss of CNTs is smaller than the impurities [114]. The reason to oxidize these impurities is more defects or open structures associated with them. This is another reason that the attachment of these impurities is often observed with a used metallic catalyst, and this metal catalyst may also play a role in oxidation [117,118,123,124,127]. There are some factors, such as type of oxidant, time of oxidation, temperature, metal contents, and environment, which can affect the oxidation efficiency and final yield.

Typically, the method of acid treatment is used to eliminate the metallic impurities associated with CNTs. First of all, by oxidizing or sonication of the CNTs, the surface of associated impurities (metals) is made apparent to acid until the solvation and finally CNTs collect in suspension. It has been observed in a number of studies that by using HNO_3 for the purpose of acid treatment, it only affects the metallic impurities rather than the CNTs or other carbon containing impurities [117,118,122,125]. By using HCl for this purpose, the impacts on CNTs and carbon impurities are also observed to a small extent [117,123,126]. Acid treatment for purification of CNTs in diluted form (4M HCl) can show same results as by the HNO_3, but the metal surface must be apparent to the applied acid to make the solvation [128].

Although purified CNTs are produced relatively by acid reflux, the nanotubes amalgamate, and the impurities that they capture are very hard or sometime impossible to remove by filtration [129]. Therefore, a surfactant-based sonication process is implemented generally by dissolving sodium dodecyl benzene sulfate (SDBS) in ethyl or methyl alcohol solution for this purpose. Since after sonication CNTs took longer to settle down, ultrafiltration is required and then annealed at a high temperature (about 1000 °C) in the presence of N_2 for 4 h. Annealing of CNTs is performed to optimize their structure. Surfactant-based sonication has been presented to be an effective method for removing tangled impurities associated with amalgamated CNTs [116].

Table 3. Typical purification technologies and their characteristics [130,131].

Technologies	Methods		Characteristics	
			Advantages	**Limitations**
Physical method	Filtration		1. Non-destructive 2. Retains the inherency and intrinsic structure necessary to elucidate the properties of CNTs 3. More suitable as an auxiliary step in combination with chemical purification 4. Improve crystallinity 5. High selectivity to metal 6. CNTs can be separated on the bases of difference in length and conductivity	1. Not very effective 2. CNT samples need to be extremely dispersed 3. Purification of samples can be done in a limited quantity at a time
	Centrifugation			
	Solubilization with functional groups			
	High temperature annealing			
	Chromatography, electrophoresis			
Chemical method	Gas phase	Air, Cl_2, H_2O, HCl, H_2O, Ar, O_2, $C_2H_2F_4$, SF_6	1. Opens the lid of the CNTs without affecting sidewalls or associated functional groups 2. Eliminates polyhedral and amorphous carbon and metallic impurities at the cost of substantial amounts of CNTs or damage to the CNT structure 3. Leads to functional groups 4. Does not disrupt or affect the alignments of CNTs	1. Low yield 2. Produces more defects on sidewalls, breaks into different shorter length, and also the alignment and structure are affected greatly, thus limiting the final applications of CNTs
	Liquid phase	HNO_3, H_2O_2, HCl, Mixture of acid or $KMnO_4$, Microwave in inorganic acid		
	Electrochemical	Alkali or acid solution		
Multi step method	Oxidation, sonication, centrifugation, filtration, wet grinding, and HIDE		1. High-purity with respect to metal 2. Metal free, improving crystallinity 3. Effectively removes carbonaceous and metallic impurities 4. Better purification yield due to the early removal of metallic impurities that can oxidize CNTs	1. Low yield
	Filtration/magnetic filtration, oxidation, annealing			
	Filtration, sonication in HNO_3, HF, H_2O_2, or SDS			
	Annealing at high temperature, extraction			

Table 4. Impurities associated with CNTs and their detection techniques.

Technique	Residual Material	Assessment Techniques	Advantages	Limitations
Thermo-gravimetric analysis (TGA)	Carbonaceous impurities Metal impurities	After oxidation of material, the residual metallic impurities are calculated by weighing ash and the carbonaceous impurities by area ratio of DTG	Accurate measurement of impurities	Completely oxidize/destroy the CNTs
Raman spectrometry	Carbonaceous impurities Structure defects Conductivity characteristics	The pure CNTs are associated with G-band by RBM as well as no D-band	Conductivity features and quality of CNTs can be measure along with their diameter	Difficult or even unacceptable for MWCNTs and metallic contents
Electron microscopy (SEM, TEM)	Defects in CNTs Amorphous carbon	Directly observes and qualitatively evaluates the adhesion defects on the CNT wall, the amount of amorphous carbon, fullerene	Absolute scrutiny can be undertaken	Can analyze the sample in a very small amount
UV–vis-NIR	Carbonaceous impurities conductivity characteristics	Absorption spectroscopy or reflectance spectroscopy in the ultraviolet-visible spectral region	Conductivity features and contents of CNTs can be analyzed exactly	A standard sample is needed with 100% purity
X-ray photoelectron spectroscopy (XPS)	Support material/functional groups (fine alumina, magnesium oxide, silica, zeolite, etc.)	Quantitatively characterizes the type and contents of functional groups or support materials	Analysis of functional groups on CNTs can be undertaken exactly	Unacceptable for purity
Energy-dispersive X-ray spectroscopy (EDS)	Metal impurities	Analytical technique used for chemical and/or elemental analysis of a sample	Contents and traces of different elements can be analyzed	Evaluation of the contents of CNTs is invalid

4. Functionalization of CNTs

The non-polar nature of graphene layers makes the CNTs naturally hydrophobic. The hydrophobic property of CNTs is indispensable for the adsorption of aromatic contaminants like benzene and anthracene. A very strong complexion is formed due to π electrons present on the graphene layer making CNTs, between aromatic contaminants and the tube surface [132]. The surface affinity of CNTs can be modulated to a variety of contaminants in water and wastewater after the purification and surface functionalization. Higher adsorption of benzene was obtained by using CNTs as compared to activated carbon (AC) because of strong interaction between benzene rings and the surface of CNTs due its hydrophobicity [133]. Figure 3 shows the different routes and schemes of CNT functionalization to increase their affinity for water and wastewater contaminates, which can be subsequently captured on the surface of CNTs used. Moreover, the functionalization of CNTs can be divided into three categories, shown in Figure 4 [134]:

1. With π conjugated network of CNTs through covalent bonds;
2. Attachment of different chemical groups via non-covalent bonds by using hydrophobicity of CNTs such as hydrogen bonds, π–π interactions, or ionic bonds;
3. Inline filling (endohedral) of hollow tubes of CNTs. The two methods are more common for CNTs functionalization and variously used by the researchers.

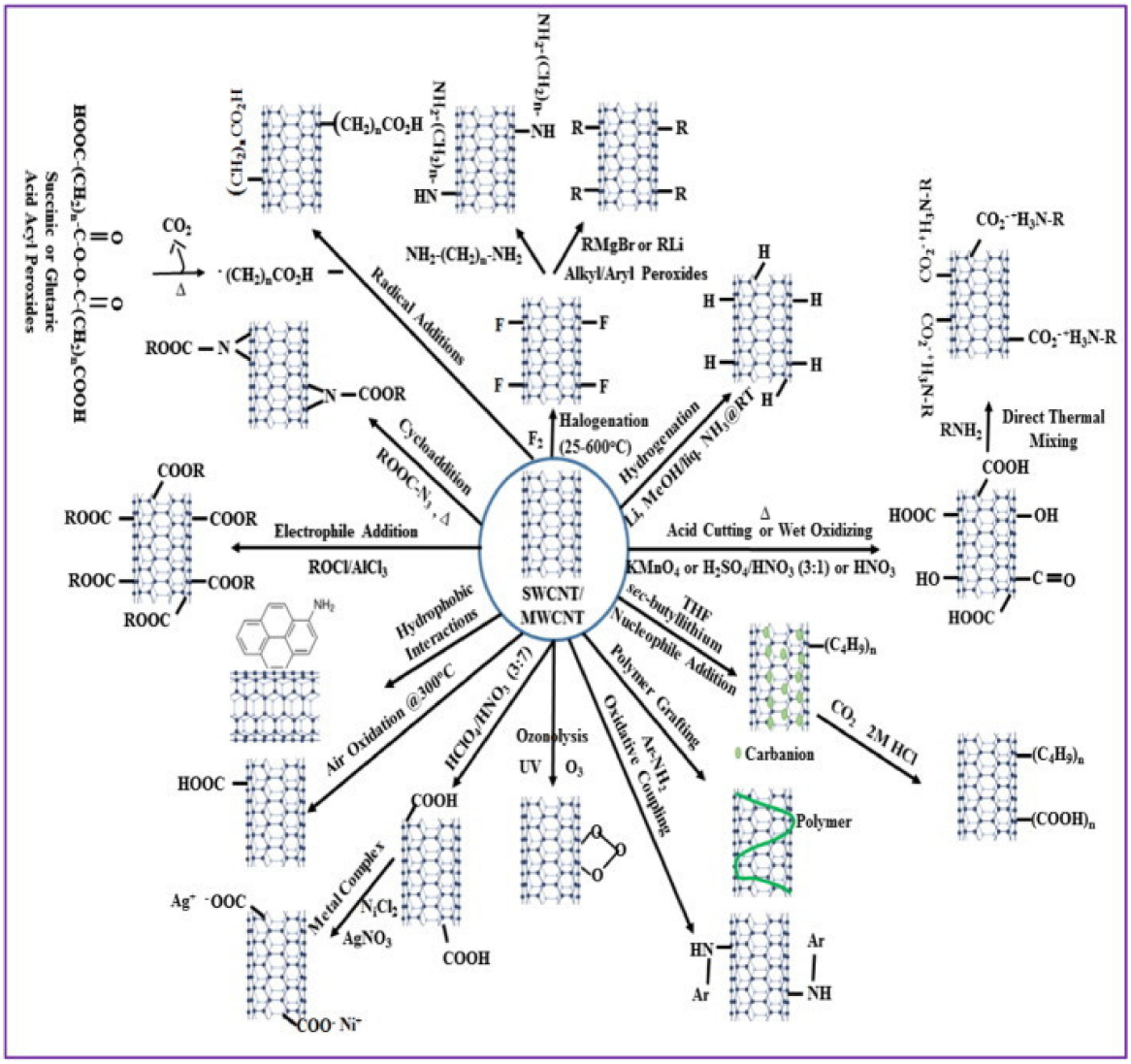

Figure 3. Functionalization routes of CNTs and associated functional groups [132].

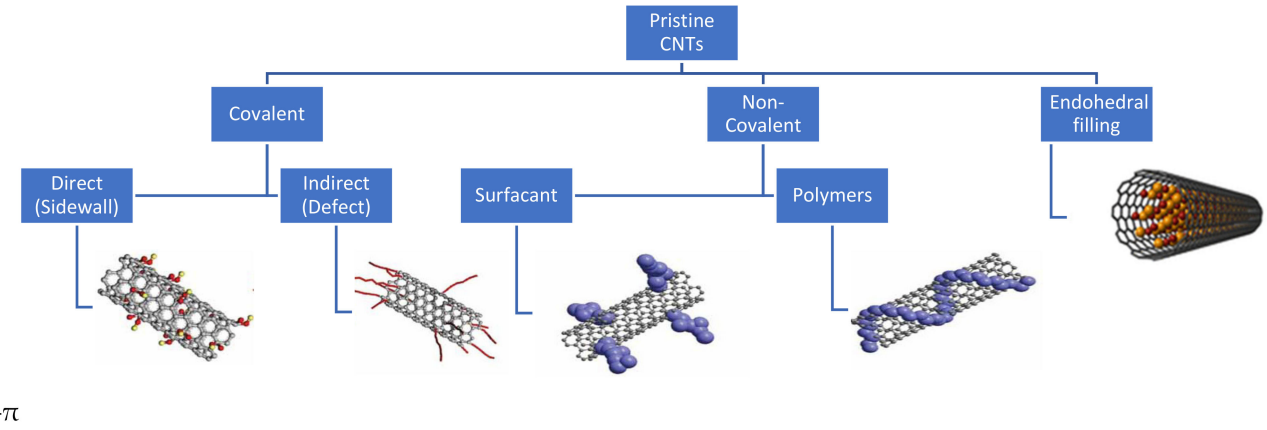

π–π

Figure 4. Methods of functionalization of carbon nanotubes.

CNTs are unique because of their distinctive properties such as adsorption capability, permeability, morphology, and physicochemical properties. There are several disadvantages that are also associated with raw CNTs, such as their low dispersion in solutions and low adsorption capacity for bulk fabrication of CNTs with organic and inorganic composites. In fact, aggregation is the main problem for low contaminant adsorption efficiencies by the original CNT samples [33,53,135–137] and also obscures the process of membrane preparation [138]. The π–π interactions and van der Waals force between CNTs are responsible for the less dispersion, which results in tight fit bundles and aggregation of CNTs [139]. As the number of graphite layers of CNTs decreases from MWCNTs to SWCNTs, the tendency to bunch increases [140]. Therefore, to overcome these drawbacks, the chemical reactivity and contaminant adsorption capacity of CNTs must be improved by increasing their dispersion rate, and this is done by functionalizing the nanotube [53,135–137,139,141]. Furthermore, solubility of CNTs can be increased by their functionalization, which causes them to repel each other [50]. Table 5 provides a compression between adoption capacities and the corresponding surface area of pristine and oxidized CNTs treated with different acids [142].

Table 5. Adsorption capacity of CNTs and corresponding surface area [142].

CNTs	Adsorption Capacity (mg/g)	Surface Area (m^2/g)
Pristine	1.1	82.2
H_2O_2 oxidized	2.6	130.0
HNO_3 oxidized	5.1	84.3
$KMnO_4$ oxidized	11.0	128.
NaOCl oxidized	47.4	94.9

Different physical or chemical processes like oxidation, impregnation, or grafting (Figure 3) are used for the functionalization of CNTs [143,144]. During the process of functionalization, the covalent or non-covalent bonds of particular functional groups result on the end or sidewall of CNTs. Functionalization is preferred over covalent bonding, because non-covalent bonding does not influence the structure and surface area of CNTs [135]. Advantages and the limitation of covalent and non-covalent functionalization of CNTs are discussed in Table 6. Functionalization is generally done to increase the dispersibility as well as contaminant removal efficiency of CNTs, thereby improving the water or wastewater treatment application capability of the CNTs or promoting membrane fabrication [145]. Higher dispersibility in polar solvent (water) was found by covalent functionalization of CNTs with the phenolic group by 1,3 dypolar cyclo addition; covalent functionalization of CNTs with phenol groups by 1, 3-dipolar cyclo-addition was found, which facilitated

CNTs' amalgamation into the polymer matrix [139]. Oyetade et al. [141] found that MWCNTs efficiently absorbed Pb^{2+} and Zn^{2+} from aqueous samples after functionalizing with nitrogen. The increase in adsorption was due to higher surface area and more adsorption sites linked to CNTs.

Table 6. Benefits and limitations of covalent and non-covalent functionalization [134].

Methods	Benefit(s)	Limitation(s)
Covalent functionalization	Highly stable bonds are formed	Intrinsic characteristics are damaged Structural defects CNTs Aggregation of CNTs
Non-covalent functionalization	Simple and easy procedure CNTs structure is maintained with minimum defects Electronic characteristics of CNTs are not affected	Stability of bonds is weak

Oxidation of raw CNTs with HNO_3, H_2SO_4, HCl, H_2O_2, $KMnO_4$, and NaOCl, or sometimes a combination of some of these (Figure 5), has often been exercised to introduce oxidized functional groups [146,147]. Generally, oxidation improves the dispersibility and enhances the ability to adsorb certain harmful contaminants in water and wastewater at the expense of fractional damage to the surface of CNTs, as described earlier. Furthermore, the surface of CNTs can also be modified with the addition of oxygen containing functional groups by performing oxygen–plasma action. In addition to oxidation and plasma action for surface modification, the CNTs can also be successfully modified with the addition of metal oxides like Al_2O_3 [148], MnO_2 [149], and Fe_3O_4 [150], which deliver another way to coat the surface of CNTs, thereby increasing the contaminant removal efficiencies of CNTs [53,135–137]. The potential surface modification schemes of CNTs used for targeted contaminants are shown in Figure 5.

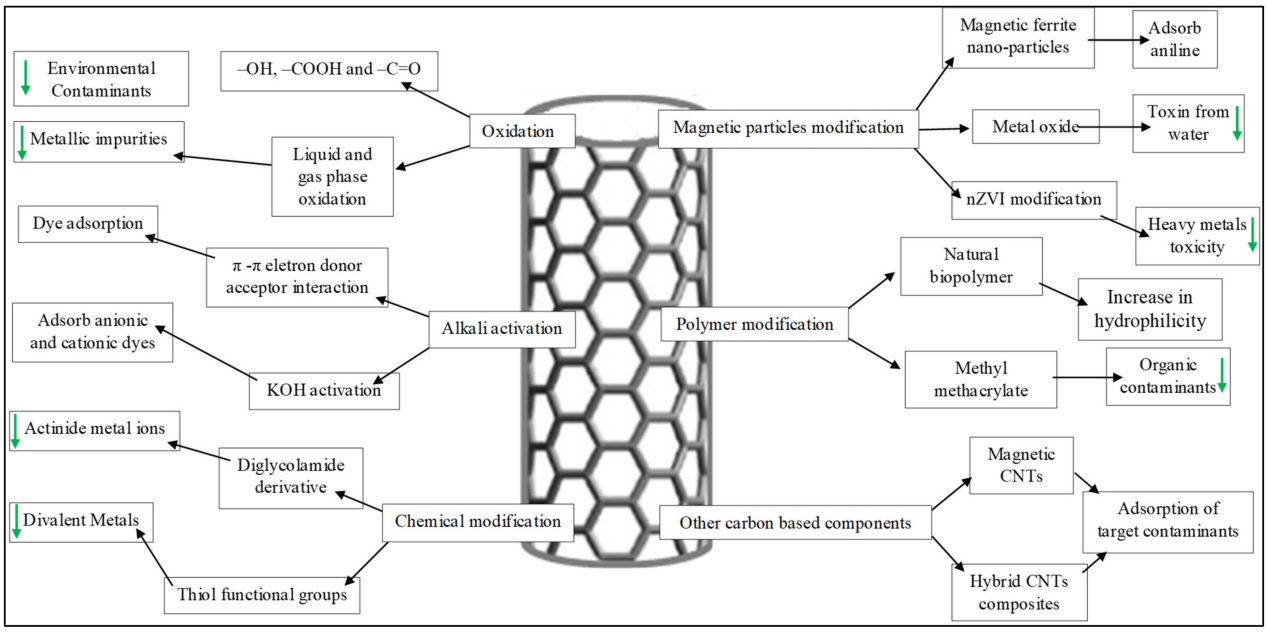

Figure 5. Schematic representation of surface modification schemes of CNTs used for targeted contaminants (green arrows refer to decrease in final effluent concentration).

5. Characterization of CNTs

Intrinsic properties of CNTs make them fascinating and desirable candidates for diverse remediation. Characterization of CNTs plays an important role due to their distinctive properties. Numerous comments and debates have been published in past decades on

different techniques and strategies used to evaluate CNTs [151–154]. Techniques used for the characterization of CNTs are divided into four groups: microscopy and diffraction, thermal, spectroscopic, and separation techniques [155]. Sometimes research includes one more group, the magnetic measurement technique. Table 7 shows different characterization techniques used for the evaluation of CNTs. It must be noted more than one technique is prominent for the characterization of CNTs; techniques employed alone are not fully characterized, nor they are absolutely quantitative. Even though qualitative analysis of CNTs can be done by electron microscopy, scanning electron microscopy (SEM) evaluates the nanostructure of the tubes, and transmission electron microscopy (TEM) is used for further precise inspection, generally detecting the defects in CNTs [129,156].

Table 7. Different analytical techniques used for the characterization of carbon nanotubes [155].

Characterization Techniques	Used for Studying
Microscopy and diffraction techniques	[157–159]
SEM	Morphological analysis (diameter and length), aggregation state
TEM/HR-TEM	Morphological analysis of internal structure (diameter, number of layers and distance between them)
AFM	Morphological analysis of internal structure (diameter, number of layers and distance between them)
Scanning tunneling microscopy	Morphological analysis of internal structure (diameter, number of layers and distance between them)
Neutron diffraction	Morphological analysis of bulk samples
XRD	Morphological analysis of bulk samples
Spectroscopic techniques	[139,160,161]
Raman spectroscopy	Purity and presence of by-products, diameter distribution, (n, m) chirality
IR and FT-IR	Purity, functionalization by attaching functional groups to the sidewall
UV–vis and NIR	Dispersion efficiency, diameter and length distribution, purity
Fluorescence spectroscopy	Size, dispersion efficiency, (n, m) chirality
XPS and EDS	Elemental composition, functionalization (covalent and non-covalent)
Thermal techniques	[162]
TGA	Purity and presence of by-products, quality control of synthesis and manufacture processes
Separation techniques	
Size exclusion chromatography	Purification, separation by size (length)
Capillary electrophoresis	Purification, separation by size (length, diameter, and cross-section)
Field flow fractionation	Fractionation by size (length)
Ultracentrifugation	Separation by chirality, electronic type, length, and enantiomeric identity
Magnetic techniques	[158,163,164]
Vibrating sample magnetometry	Magnetic properties
Alternating gradient magnetometry	Magnetic properties
Superconducting quantum interference device	Magnetic properties

The ultrastructure of different types of species including organic, inorganic, and biological species can be evaluated by using very popular techniques known as SEM and TEM. The scanning of the sample in SEM generates an image when the targeted electron ray interacts with sample of CNTs. Generally, the technique is used to analysis the morphology (length and diameter) of nanomaterials [123,155,165] to assess the quality of prepared CNTs. For example, Figure 6a shows a SEM image of the as-prepared CNTs [148], and Figure 6b

shows alignment of CNTs synthesized by using a horizontal quartz tube housed in muffle furnace. Average length of the tubes was 70 µm measured by using SEM [166]. Sometimes, it is also used to validate the surface modifications in terms of functional reactions that occur on the surface of CNTs [167]. In the case where the required measurement exceeds 1 to 20 nm resolution while using SEM, then TEM is used [156,167]. Small dimensions in CNTs such as interlayer distance, diameter, and number of graphene sheets can be easily examined (Figure 6c,d) by targeting the sample with a high energy electron beam of up to 300 keV [168,169]. It should be noted that the functional groups (organic and inorganic) that modify the surface of CNTs can also be evaluated by using TEM [161,170,171]. Moreover, structural integrity, surface functionalization, and defect son the surface of CNTs caused by the oxidation (acidic or basic) to introduce oxygen containing functional groups like hydroxyl, carbonyl, and carboxylic acid groups have also been studied by using both SEM and TEM techniques [155,172].

The image of the atomic structure and crystal structure information can be obtained by using high resolution transmission electron microscopy (HR-TEM) [173]. A high phase contrast image as small as the crystal unit can be obtained. This technology is widely used for advanced characterization of materials, allowing access to information on just-in-time defects, stacking faults, deposits, and grain boundaries. In addition to the morphology of the MWCNTs in the HR-TEM image, the direct measurements can be made on the MWCNT walls. For example, the number of walls constituting the nanotubes can be directly counted and recorded as control parameters in subsequent experiments in case the number of such walls needs to be changed. In addition, the interplanar distance between the walls can be accurately measured and compared with the crystal structure data table of the carbon structure and its respective diffraction pattern.

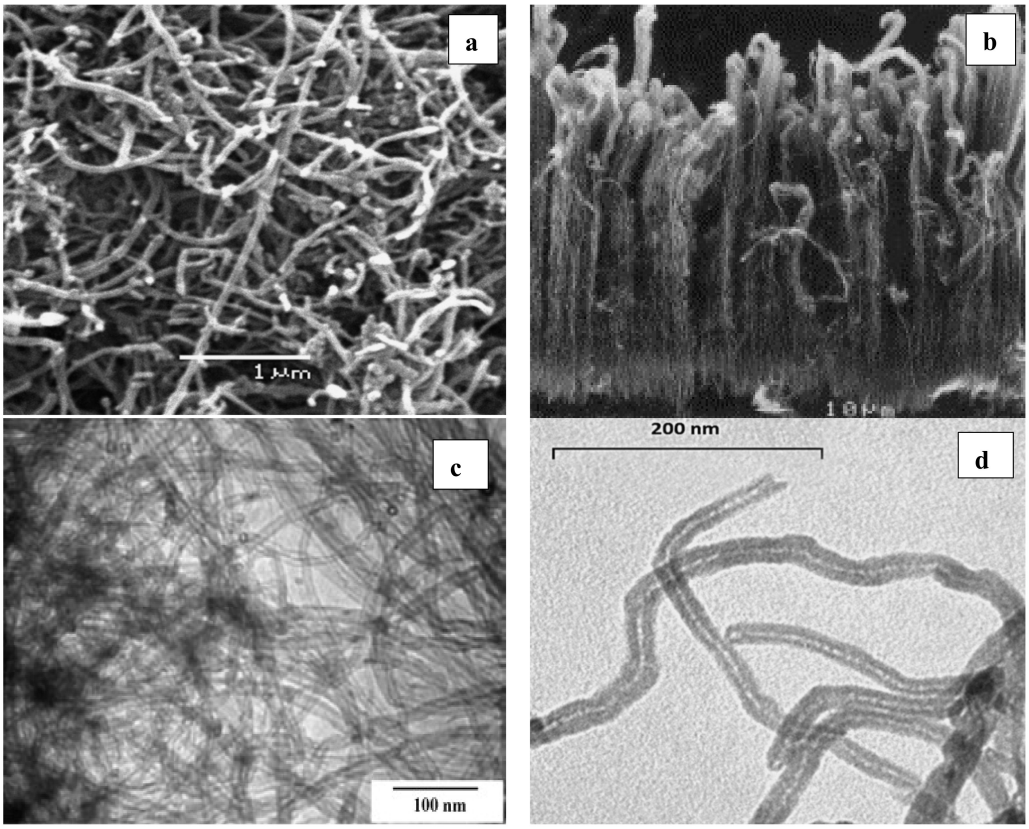

Figure 6. (**a**) SEM image of a bulk sample of multi-walled carbon nanotubes [155], (**b**) SEM image showing vertical aligned CNTs [174], (**c**) high-magnified TEM images of CNTs grown on unreduced catalyst [168] and, (**d**) TEM image of a bulk sample of multi-walled carbon nanotubes [155].

The chemical state and structure of CNTs can be obtained by using an X-ray photoelectron spectroscopy (XPS) technique [114]. However, the data obtained from this technique are used to examine the structural modification of CNTs before and after the chemical interactions with organics, inorganics, or gaseous adsorption. The investigation of CNTs by using XPS is done after the incorporation of nitrogen into the nanotube [175]. Due to the polar nature of the carbon–nitrogen bond, the peak shift before and after the modification is evidence of nitrogen incorporation [176,177]. Furthermore, the technology demonstrates that carbon nanofibers are more similar to carbon oxides than various graphites [178]. Fluorinated functionalization of SWCNTs was also studied by using XPS; the results concluded that three peaks of sp^2, sp^3, and carboxyl groups (284.3, 285, and 288.5 eV, respectively) were associated with C1s of un-doped nanotubes [114]. The observed carboxyl group (288.5 eV) was similar to in nanofibers [179].

Crystallinity of CNTs can be obtained by using an X-ray diffraction (XRD) technique [90,176]. X-ray diffraction patterns of graphite and CNTs are very close to each other because of their inherent properties. The XRD pattern of CVD-synthesized MWCNTs is shown in Figure 7, illustrating a peak similar to graphite (002), and the measured layer spacing can be obtained from Bragg's law, while the other peaks (family of (hk 0) peaks)) can be obtained because the mono-graphene layer makes the honeycomb matrix [114]. Therefore, the curve obtained by XRD does not distinguish between the microstructure information of CNTs and graphite; nevertheless, it is helpful for purity analysis of the sample [102,103]. The XRD pattern revealed that straight CNTs with a good alignment on the surface of the substrate did not show the peak, i.e., 022 [114]. For CNTs aligned vertically to their substrate surface, the XRD pattern is not collected because of the scattering of the beams inside the sample. Therefore, the 002 peak is always lowered for better-aligned CNTs [180]. In addition, several other types of parameters such as bundle size, mean diameter, and diameter dispersion can also be studied by using the XRD technique. The peak 10 is greatly influenced by these parameters in terms of its location and thickness [181,182].

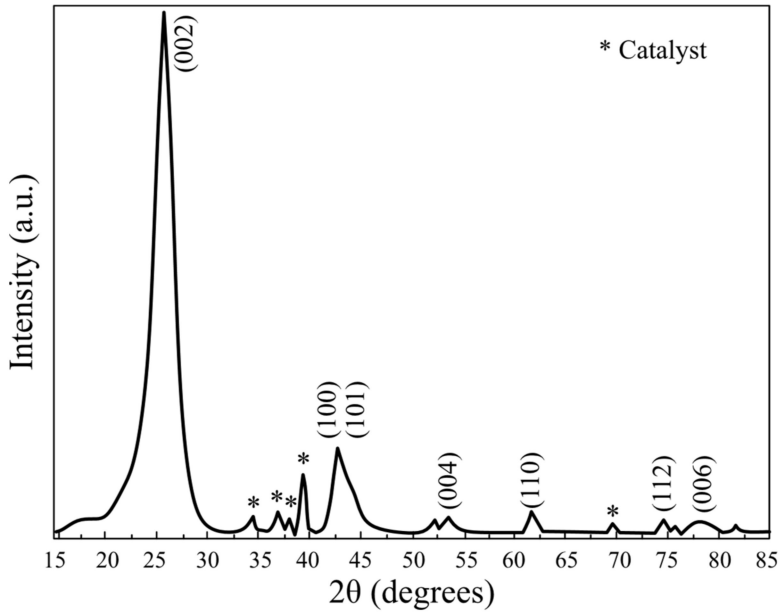

Figure 7. XRD pattern of MWCNTs synthesized by CVD [114].

Qualitative evaluation for nanotubes' surface can be done by using Fourier transform infrared spectroscopy (FT-IR) [183]. The sample is characterized by passing the infrared radiations through it, and the part of radiations absorbed by the sample at specific energy is determined. Each functional group is identified by a particular range of frequency with associated absorption peaks. The infrared spectrum of the original CNTs (Figure 8) shows a characteristic band of about 1600 cm^{-1} associated with aromatic rings (C=C bond) of

rolled graphene layers. Sometimes, the peaks of 3800 to 3200 cm^{-1} (O-H stretch) and 1700 particles that absorb moisture into the atmosphere or due to certain purification processes [184]. In addition, a band of 2910 to 2940 cm^{-1} was also detected for CNTs, which is related to the vibration of C-H stretching methylene (CH_2) [185]. The FTIR spectra can also suggest surface modification of CNTs. For example, in Figure 8b, a new peak near 1450 cm^{-1} appeared that was assigned to asymmetric CH_2 bending. This peak is typically interpreted as evidence of defects in the structure of CNTs. In Figure 8c, a new peak near 1735 cm^{-1} suggested a carbonyl stretch of the carboxylic acid group. In addition, a double peak at approximately 2900 cm^{-1} was attributed to the loss of aromaticity due to the oxygen functional groups.The thermal stability and proportion of volatile compounds of nanotubes can be analyzed by an analytical technique called thermogravimetric analysis (TGA). The analysis is made by heating the sample directly in the air or inert gases (He/Ar) while recording the change in its weight with respect to elevated temperature [176,186,187]. In some cases, the analysis is made in the presence of N_2 or He with poor oxygen atmosphere (1% to 5% O_2) to slow oxidation [188]. During the TGA analysis of the CNT sample in the air atmosphere, the weight loss of the sample (Figure 9) is usually due to carbon oxidation to CO_2, while the solid oxides after the oxidation of metallic catalyst are responsible for the superposition of the sample [165,189,190]. Generally, the percent yields of carbon deposits are determined by using TGA. Usually, during the oxidation of the sample the weight occurs in the temperatures ranging from 200 to 680 °C [190]. The contents of carbon can be calculated by obtaining the percentage of $(m_1 - m_2)/m_1$, where m_1 is the weight of the sample before oxidation and m_2 is the weight of the sample after the oxidation [11].

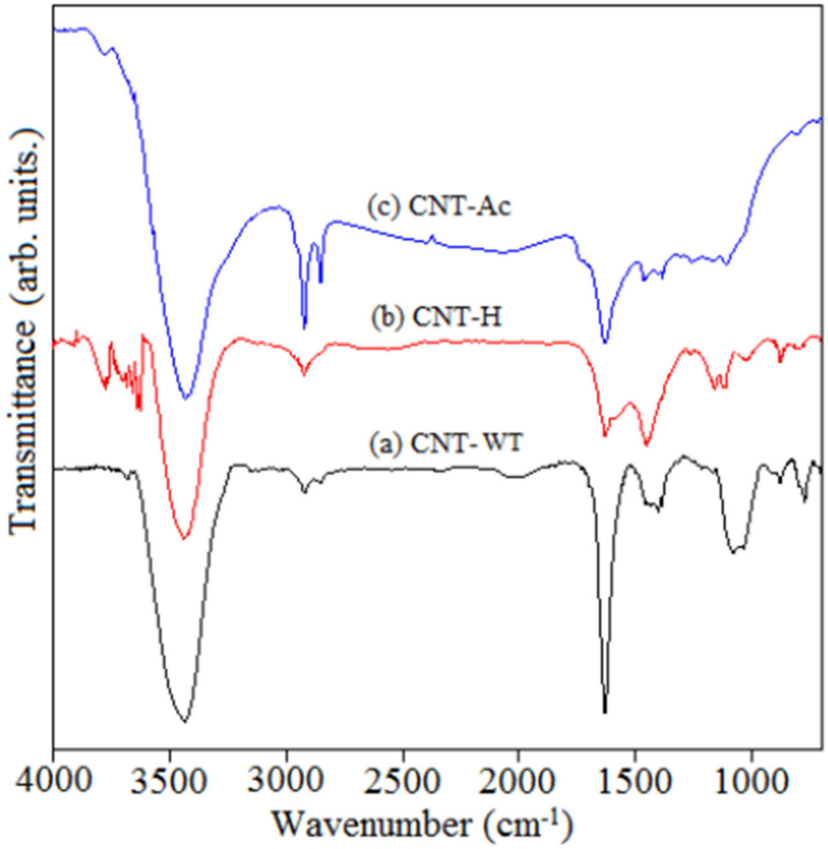

Figure 8. FT-IR spectra of CNTs: (a) pristine CNTs (CNTs-WT), (**b**) CNTs treated with HCl (CNT-H), and (**c**) CNTs treated with mixture of H_3SO_4 and HNO_3 (CNTs-AC) [191].

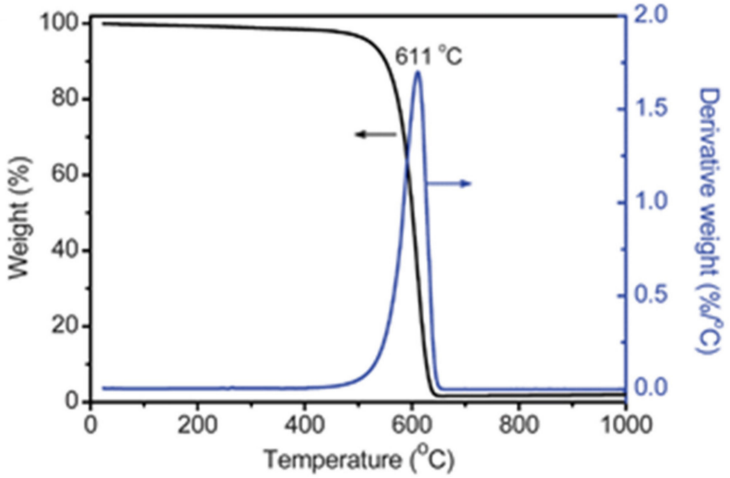

Figure 9. TGA analysis of the CNT sample [190].

The structural features of CNTs can be defined by their crystalline structure, chiral carrier, and single- or multi-walled features [192]. Crystalline arrangement of nanotubes can be characterized by the ID/IG ratio determined from the RAMAN spectroscopy. ID/IG indicates the ratio between the organized and unstructured carbon in the CNTs and uses the intensity of defective and graphitic carbon (D and G bands) at the high wavenumbers in the RAMAN absorption spectrum (Figure 10) [193]. ID/IG is a good quality indicator for CNTs, and the low ID/IG ratio is characteristic of highly graphitized structures; the laboratory reported mass of MWCNT is 0.65, and industrial grade MWCNT is 2.04 [90,194].

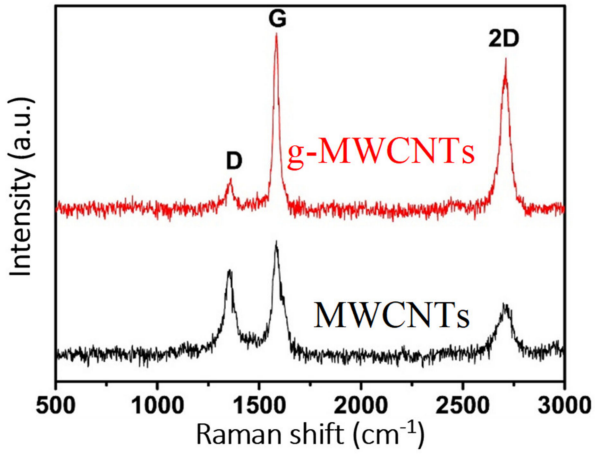

Figure 10. Raman spectra of pristine (MWCNTs) and graphitized MWCNTs (g-MWCNTs) [193].

6. Applications of CNTs

6.1. Removal of Heavy Metals

Removal of heavy metals from water and wastewater by using surface modified CNTs has been studied extensively [143,195–197]. Contaminant adsorption mainly occurs at four possible types of sites that are available on the CNTs such as outer and inner grooves and interstitial channels mas shown in Figure 11, but the inner region of the nanotubes is less adsorbed [53,135–137,198]. Bahgat et al. [143] used functionalized MWCNTs for the adsorption of heavy metals and concluded that adsorption of the metals occurs because of a number of adsorption spots available on the tubes' surfaces. In another study, higher adsorption of Zn^{2+} ions was observed by the plasma-treated CNTs due to the availability of more oxygen-containing functional groups. The mechanism of surface complexation was responsible for the adsorption of cationic ions, as the adsorption sites increased due to deprotonating functional groups [197].

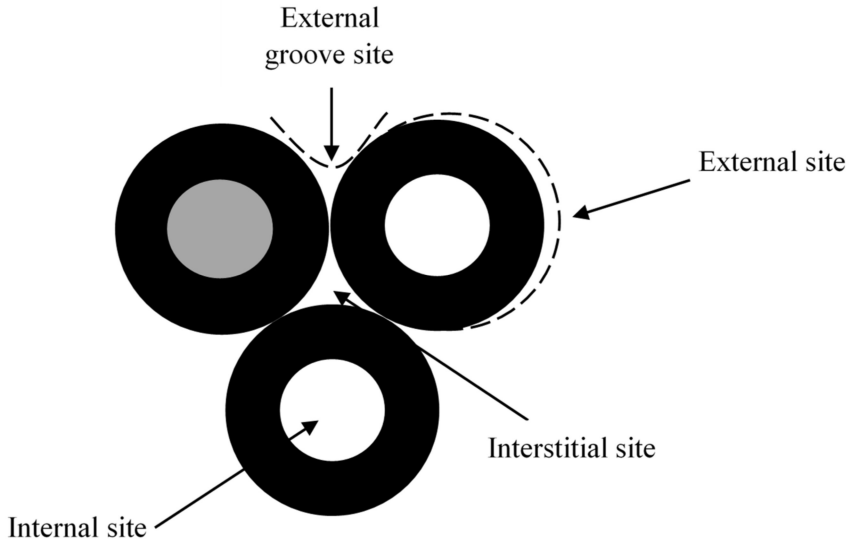

Figure 11. Different adsorption sites on CNTs [198].

Surface modification of CNTs improved their affinity for heavy metal ions and metalloid adsorption [199,200] by incorporating iron oxide and oxidation [16,201–203], coating with oxides of nonmagnetic metals [204], introducing a thiol functional group [82], and functionalizing with sulfur [205]. According to Addo Ntim and Mitra [203], the different oxides of iron such as magnetite (Fe_3O_4), maghemite (γ-Fe_2O_3), hematite (α-Fe_2O_3), and goethite (α-FeO) are very useful for the removal of trace heavy metals present in water and wastewater [170].

Generally, the process of surface modification of functionalization of CNTs is responsible for the adsorption mechanisms of heavy metals [53,191,206]. Table 8 shows an explanation of previously used functionalized CNTs and their adsorption capacities and removal mechanisms. Surface area, porous structure, functional groups, and interaction mechanisms between the absorbate and absorbents are the main attributes of CNTs for their heavy metal adsorption capability [53,136,137,143]. In addition, these properties enhance the heavy metal removal efficiencies onto the polymer film incorporated by functional CNTs [135].

Physical and chemisorption mechanisms of adsorption have been observed between the CNTs modified with metal oxides and heavy metal ions [203]. In addition, the contaminant with particular hydration energy, ionic radius, and potential of hydrolysis also affects the adsorption capacities of CNTs. A study conducted by Hu et al. [207] confirms the above statement, when higher removal of Pb^{+2} was observed than Cu^{+2} by using MWCNTs modified with iron oxide under the same experimental conditions. The adsorption performance of CNTs for heavy metals is also affected by the presence of other organics. For example, enhanced removal of Cd^{+2} ion was observed by using oxidized MWCNTs in the presence of 1–naphthol, while there was no effect recorded during the presence of Cd^{+2} ion on the removal of 1–naphthol in similar conditions [208]. These types of results mainly occur because of the distinct interaction mechanisms that are responsible for the adsorption of different types of pollutants [170].

Solution pH also plays an important role in the adsorption capacity and mechanisms of CNTs. For example, higher pH is favorable for endospheric interactions, while the lower pH facilitates extracellular interaction and/or ion exchange of targeted metal ions and surface functional groups of CNTs [208]. Moreover, as the pH increases (alkaline conditions), the charge density of functionalized CNTs moves towards more negativity, which is efficient for the adsorption of cationics, while, at lower pH (acidic conditions), because of protonating functional groups, the positive charge density increases, which repels the cationic metals, resulting in the lower efficiency of CNTs [53,136,137]. In a study, oxidized and ethylenediamine-doped MWCNTs were used for the adsorption of

Cd^{+2} ions from aqueous samples. The results concluded that both types of absorbents removed Cd^{+2} ions strongly depending on pH ranging from 8 to 9 [209]. According to Rao and coworkers [146], the best adsorption capacity of nanotubes was observed in the pH ranging from 7 to 10. In addition to this particular range of pH, the ionization and competition between different species may also happen [210–213]. For example, an effective adsorption of Pb^{+2} ions on functionalized CNTs was reported during the co-existence of sodium dodecylbenzenesulfonate (DBS), while the adsorption of lead was significantly reduced in the presence of benzalkonium chloride [214]. The higher adsorption of lead ions might be due to anionic surfactant formation between Pb^{+2} and DBS, which are very complex compounds. In addition, the charge density (negative or positive) on the surface of CNTs makes the different interaction mechanisms of metal ions. For example, chemical interaction occurred between the N-dopped magnetic CNTs and Cr(III), while an electrostatic interaction was observed between the acid oxidized CNTs and Cr(III) [215].

Regardless of the costs, the CNTs are more efficient in terms of their adsorption and desorption phases than the AC, as reported in many studies [146,216]. Lu and coworkers [216] reported a slight decrease in adsorption and desorption of Ni^{+2} while using CNTs, and on the other hand, a sharp decrease was observed in the case of AC [216].

The adsorption of heavy metals by the functional CNTs depends on the interactions between available functional groups on the surface of CNTs and particular contaminants rather than the size of nanotubes. For example, higher adsorption of As(III) and As(V) was reported by Addo Ntim and Mitra [203] by using zirconia-modified CNTs of the same diameter (20 to 40 nm) than by using the CNTs coated with iron oxide. These results demonstrate higher arsenic adsorption by zirconia nanocomposites than the CNTs modified with iron oxide with similar range of diameters. Therefore, based on these results, further investigations on the adsorption capacities of functionalized CNTs are needed in terms of their surface area rather than the size CNTs.

Table 8. Functional CNT based nanomaterials used for the removal of heavy metal ions from aqueous samples.

Adsorbate	Adsorbent	Surface Area (m^2/g)	Diameter (nm)	Q_e/RE	Experimental Conditions			Removal Mechanism	Model	Comments	Ref.
					pH	IC	AL				
As(III)	MWCNTs	9.1	10–40	91%	6	40 µg/L	2.0 g/L	Liquid film diffusion, ion exchange	Tempkin, Dubinin-Radushkevic, Langmuir, Freundlich	In column operation, the removal As(III) was up to 13.5 µg/L	[217]
	Zero-valent iron-doped MWCNT	-	-	200 mg/g	4	10 mg/L	0.2–4.0 g/L	Ion exchange, surface complexation	Langmuir	Maximum As(III) removal efficiency was 98.5%	[218]
	Floating catalyst CNTs (FCNT)	74	18.6	1.22 mg/g	6.5	0.1–10 mg/L	1 g/L	Electrostatic attraction, surface complexation	Langmuir	Potential adsorbent for removal to total arsenic	[219]
	Oxidized-FCNT	129	10.7	1.90 mg/g							
	Heat-treated oxidized CNTs (FCNT-HOX)	168	7	5.99 mg/g							
	Zero-valent iron immobilized on MWCNTs	78.78		111.1 mg/g	7	0.1–1 mg/L	0.05 g	Surface complexation	Langmuir	Reusability of adsorbent was up to 5 cycles	[219]
	MWCNT-ZrO_2	152	20–40	2 mg/g	6	100 µg/L	100 mg/10 mL	Chemisorption/ physisorption	Langmuir	The adsorption capacity of AS (III) is not associated with pH value	[203]
	Iron-oxide-coated multi-walled carbon nanotubes	153	20–40	1.723 mg/g	4	100 µg/L	10 mg/10 mL	Electrostatic interaction, surface complexation	Langmuir	Suggesting that modifying MWCNTs with other groups can develop potential adsorbents for water treatment	[203]

Table 8. *Cont.*

Adsorbate	Adsorbent	Surface Area (m^2/g)	Diameter (nm)	Q_e/RE	Experimental Conditions			Removal Mechanism	Model	Comments	Ref.
					pH	IC	AL				
As(V)	Iron-oxide-coated SWCNTs	-	-	49.65 mg/g	4	5–50 mg/L	-	Surface complexation	Freundlich	Adsorption was very fast for low concentration of As(V)	[220]
	MWCNTs	9.1	10–40	92%	6	40 µg/L	2.0 g/L	Liquid film diffusion, ion exchange	Tempkin, Dubinin-Radushkevic, Langmuir, Freundlich	In column operation, the removal As(III) was up to 14.0 µg/L	[217]
	Zero valent iron doped MWCNTs	-	-	250 mg/g	4	10 mg/L	0.2–4.0 g/L	Ion exchange, surface complexation	Langmuir	Maximum As(V) removal efficiency was 98.5%	[218]
	Floating catalyst CNTs (FCNT)	74	18.6	0.88 mg/g	6.5	0.1–10 mg/L	1 g/L	Electrostatic attraction, surface complexation	Langmuir	Potential adsorbent for removal to total Arsenic	[219]
	Oxidized-FCNT	129	10.7	2.51 mg/g							
	Heat-treated oxidized CNTs (FCNT-HOX)	168	7	6.37 mg/g							
	3-(2-aminoethylamino) propy-ltrimethoxysilane modified MWCNTs	-	-	8.01 mg/g	2.2	1.0 mg/L	40 mg	-	-	Cr(IV) was selectively adsorbed in the micro-column packed with adsorbent	[221]
	Zero-valent iron immobilized on MWCNTs	78.78		167 mg/g	7	0.1–1 mg/L	0.05 g	Surface complexation	Langmuir	Successfully applied to ground water with high pH	[219]

Table 8. *Cont.*

Adsorbate	Adsorbent	Surface Area (m^2/g)	Diameter (nm)	Q_e/RE	Experimental Conditions			Removal Mechanism	Model	Comments	Ref.
					pH	IC	AL				
	Iron(III)-oxide-coated ethylenediamine functionalized MWCNTs	198.5	5–10	23.5 mg/g	4	100 µg/L	50 mg/10 mL	Ion exchange	Langmuir	Greater efficiency to remove As(V) due to enormous adsorbing sites	[222]
	MWCNT–zirconia nanohybrid	152	20–40	5.0 mg/g	6	100 µg/L	100 mg/10 mL	Chemisorption/ physisorption	Langmuir	The adsorption capacity of As(V) is not associated with pH value	[223]
	Iron-oxide-coated MWCNTs	153	20–40	0.189 mg/g	4	100 µg/L	10 mg/10 mL	Electrostatic interaction, surface complexation	Langmuir	Modifying MWCNTs with other groups can develop potential adsorbents for water treatment	[203]
Cr(III)	Iron oxide/carbon nanotubes/chitosan magnetic composite film	64.4		66.25 mg/g	2–10	100 mg/L	0.3 mg/g	Electrostatic	Langmuir	Decrease in efficiency was 12% after reusing the adsorbent for ten cycles	[224]
	Nitrogen-doped magnetic carbon nanoparticles	-	-	83.7 mmol/g	8	200 mg/L	10 mg/500 mL	Chemical adsorption	Langmuir	10-fold greater removals than activated carbon due to large SSA	[225]
	Acid modified MWCNTs	-	23	0.5 mg/g	7	1 mg/L	120 mg/500 mL	Electrostatic interaction	Pseudo-second order	Increasing removal of Cr with increasing the dose of CNTs	[215]

Table 8. *Cont.*

Adsorbate	Adsorbent	Surface Area (m^2/g)	Diameter (nm)	Q_e/RE	Experimental Conditions			Removal Mechanism	Model	Comments	Ref.
					pH	IC	AL				
Cr(IV)	Iron oxide/carbon nanotubes/chitosan magnetic composite film	64.4	-	449.3 mg/g	10-Feb	100 mg/L	0.3 mg/g	Electrostatic	Langmuir	Decrease in efficiency was 6% after reusing the adsorbent for ten cycles	[224]
	Nitrogen-doped magnetic CNTs	116.4	-	970.9 mg/g	1	40–1000 mg/L	0.5–3.5 g/L	Surface complexation	Langmuir	Recycled adsorbent was successfully used for excellent electrochemical reduction of CO_2	[163]
	Chitosan-modified MWCNTs	-	30–50	164.0 mg/g	2	50 mg/L	50 mg	Electrostatic	Langmuir	Adsorbent can be recycled up to 4 times	[226]
	Magnetic iron oxide MWCNTs	-	~50	42.0 mg/g	2	5 mg/L	0.4–1.0 g/L	Electrostatic	Langmuir	Absorbent highly showed durability, selectivity, easy regeneration ability	[227]
	Chitin magnetite MWCNTs	69.1	-	100%	2	50 mg/L	-	Physical	-	Removal of Cr(IV) was enhanced after mixing MWCNTs with chitin	[228]

Table 8. *Cont.*

Adsorbate	Adsorbent	Surface Area (m^2/g)	Diameter (nm)	Q_e/RE	Experimental Conditions			Removal Mechanism	Model	Comments	Ref.
					pH	IC	AL				
	Magnetic MWCNTs	200	20–40	16.23 mg/g	3	25 mg/L	-	-	Langmuir	The adsorption capacity of adsorbent increases with initial concentration of Cr(VI) and contact time, but decreases with the increase of adsorbent dosage	[229]
	3-(2-aminoethylamino) propyltrimethoxysilane-modified MWCNTs	-	-	9.79 mg/g	2.2	1.0 mg/L	40 mg	-	-	Cr(IV) was selectively adsorbed in the micro-column packed with adsorbent	[221]
	Activated-carbon-coated CNTs	-	10–20	9.0 mg/g	2	0.2–0.5 mg/L	2 mg/50 mL	-	Langmuir	The f-CNT can be used largely for the removal of Cr ions	[215]
	Ceria-supported CNTs nanoparticles	-	20–80	31.55 mg/g	7	35.3 mg/L	100 mg/100 mL	Ion exchange	Langmuir	Suggesting that CeO_2/ACNTs has high potential for heavy metal removals	[230]

Table 8. *Cont.*

Adsorbate	Adsorbent	Surface Area (m^2/g)	Diameter (nm)	Q_e/RE	Experimental Conditions			Removal Mechanism	Model	Comments	Ref.
					pH	IC	AL				
Pb(II)	Thiol-functionalizedM-WCNTs/Fe_3O_4	97.367	-	65.4 mg/g	6.5	50 mg/L	100 mg/100 mL	Lewis acid–base interactions	Langmuir	The adsorbent removed heavy metal ions effectively at various pH values	[231]
	Magnetic MWCNTs	295.4	-	N/A	6	100 mg/L	1000 mg	-	Experimental	High removal efficiency due to intrinsic properties, large SSA, and porous structure	[232]
	MWCNTs/Fe_3O_4	108.37	10–20	22.04 mg/g	5.3	30 mg/L	500 mg/1000 mL	Electrostatic, hydrophobic, and π–π interactions	Langmuir	Easily regenerate the adsorbent by external magnetic field after several cycles	[233]
	MWCNTs/Fe_3O_4 modified with 3-aminopropyltrie-thoxysilane	90.68	10–20	75.02 mg/g	5.3	30 mg/L	500 mg/1000 mL	Electrostatic, hydrophobic, and π–π interactions	Langmuir	Easily regenerate the adsorbent by external magnetic field after several cycles	[233]
	MWCNTs grafted/PAAM membrane	-	-	98%	-	10 mg/L	1000 mg/1000 mL	Electrostatic interaction	-	The f-CNT membrane potentially enhances the water flux and removal of heavy metals	[234]

Table 8. *Cont.*

Adsorbate	Adsorbent	Surface Area (m^2/g)	Diameter (nm)	Q_e/RE	Experimental Conditions			Removal Mechanism	Model	Comments	Ref.
					pH	IC	AL				
	Oxidized CNT sheets	-	-	117.65 mg/g	7	1200 mg/L	50 mg/25 mL	Chemical interaction	Langmuir	Considering the oxidize CNT sheets promising nanomaterial for adsorption	[235]
	MWCNTs grafted with 2-Vinylpyridine	-	-	37.0 mg/g	6	10 mg/L	640 mg/1000 mL	Ion exchange, electrostatic interaction	Langmuir	Showed high suitability for preconcentration and immobilization of heavy metal ions from water	[236]
	Oxidized MWCNTs	142.29	10–30	0.021 mmol/g	4.1	0.83 mmol/L	0.75 g/L	Chemical, electrostatic, hydrophobic, and π–π interactions	Langmuir	High removal efficiency toward heavy metal ions in wastewater	[214]
	Alumina-coated MWCNTs	-	-	99%	Different	-	10 mg/25 mL	N/A	-	The composite can be used largely to remove lead from industrial wastewater. Adsorption efficiency increased with the pH (3 to 7)	[236]
	Nitrogen-doped magnetic carbon nanoparticles		-	6.74 mmol/g	8	200 mg/L	10 mg/500 mL	Chemical adsorption	Experimental	High removal efficiency toward Pb compared to Cr	[225]

Table 8. *Cont.*

Adsorbate	Adsorbent	Surface Area (m^2/g)	Diameter (nm)	Q_e/RE	Experimental Conditions			Removal Mechanism	Model	Comments	Ref.
					pH	IC	AL				
	Titanium Dioxide /MWCNT composites	-	-	137.0 mg/g	6	10 mg/L	20 mg/10 mL	-	Langmuir	Important adsorption ability to remove large amount of Pb(II) in short period	[204]
Pb(II)	Oxidize MWCNTs	-	20–30	-	-	10 mg/L	3000 mg/1000 mL	-	-	The sorption of Pb largely depends on foreign ions and ionic strength	[237]
	Manganese oxide-coated CNTs	275	2.60	78.74 mg/g	5	30 mg/L	50 mg/100 mL	Electrostatic interaction, surface complexation	Langmuir	300% greater adsorption capacity than raw CNTs	[238]
	Acidified MWCNTs	237.3	29.0	85 mg/g	5	50 mg/L	25 mg/50 mL	Physical adsorption	Langmuir	The regeneration of Pb increasing with decreasing pH and can be used for several cycles	[239]
Cd(II)	Alumina-decorated MWCNTs	109.8	10–20	27.21 mg/g	7	1 mg/L	50 mg/L	Electrostatic interaction, physical adsorption, surface precipitation	Langmuir	Capable of removing both metallic and organic Contaminants	[240]

Table 8. *Cont.*

Adsorbate	Adsorbent	Surface Area (m^2/g)	Diameter (nm)	Q_e/RE	Experimental Conditions			Removal Mechanism	Model	Comments	Ref.
					pH	IC	AL				
	Oxidized MWCNTs	78.5	16.09	24.15 mg/g	-	5 mg/L	1 mg/10 mL	Chemisorption	Langmuir	The sorption capacity is strongly dependent on pH due to surface charge and showed best performance in the pH ranging from 6 to 10	[209]
	Ethylenediamine-functionalized MWCNTs	101.2	21.25	25.7 mg/g	-	5 mg/L	1 mg/10 mL	Chemisorption	Langmuir	The sorption capacity is strongly dependent on pH due to surface charge and showed best performance in the pH ranging from 6 to 10	[209]
	Oxidized CNT sheets	-	-	92.59 mg/g	7	1200 mg/L	50 mg/25 mL	Chemical interaction	Langmuir	Excellent removal of heavy metal ions	[235]
	Acid-modified CNTs	170	10–20	4.35 mg/g	7	-	50 mg	Electrostatic interaction	Langmuir	Potential material for water purification	[241]
	MWCNTs modified with Chitosan	-	60–100	-	-	-	2000 mg	Electrostatic interaction	-	The removal efficiency increases with increase of mass of both MWCNTs and chitosan	[242]

Table 8. *Cont.*

Adsorbate	Adsorbent	Surface Area (m^2/g)	Diameter (nm)	Q_e/RE	Experimental Conditions			Removal Mechanism	Model	Comments	Ref.
					pH	IC	AL				
Hg(II)	MnO_2-coated CNTs	110.4	30–50	58.82 mg/g	5–7	10 mg/L	200 mg/20 mL	Electrostatic interaction	Langmuir	Higher adsorption affinity to other heavy metals rather than Hg	[149]
	Thiol-derivatized SWCNTs	-	-	131.58 mg/g	5	40 mg/L	0.25 mg/mL	Electrostatic interaction	Langmuir	Easily desorb/regenerate Hg after treatment of water	[243]
	Amino and thiolated functionalized-MWCNTs	-	5–10	84.66 mg/g	6	100 mg/L	60 mg	Physisorption	Langmuir	Highly efficient removal from real wastewater and further research is necessary to commercialize	[244]
	Iodide-incorporated MWCNT (CNT-I)	153	10–20	123.45 mg/g	6	100–500 mg/L	2500 mg/1000 mL	Ion exchange	Langmuir	Successfully used for the adsorption and desorption of Hg(II)	[205]
	Sulphur-containing CNTs	-	-	72.8 µg/g	12.15	0.1mg/L	100 mg/20 mL	Chemisorption	Freundlich	Greater treatment ability for industrial wastewater containing Hg and other anions and cations	[245]
Hg(II)	Thiol-functionalized-MWCNTs/Fe_3O_4	97.2	-	65.52 mg/g	6.5	50 mg/L	1000 mg/100 mL	Lewis acid–base interactions	Langmuir	Better removal of heavy metals in different pH concentration	[231]

Table 8. *Cont.*

Adsorbate	Adsorbent	Surface Area (m^2/g)	Diameter (nm)	Q_e/RE	Experimental Conditions			Removal Mechanism	Model	Comments	Ref.
					pH	IC	AL				
	Oxidized MWCNTs	-	-	3.83 mg/g	7	10–100 µg/L	25 mg/50 mL	Electrostatic interaction	Langmuir	Small diameter of CNTs removing greater amount of Hg(II) from aqueous solution	[246]
Zn(II)	Functionalized MWCNTs	250	10–25	2.42 mg/g	10	1.1 mg/L	0.09 g	Electrostatic interaction	Langmuir	Excellent potential for the removal of heavy metal ions	[247]
	Oxidized CNTs	-	-	74.63 mg/g	7	1200 mg/L	50 mg/25 mL	Chemical interaction	Langmuir	Economically feasible material with excellent heavy metal ion removal efficiency without any CNTs leakage	[235]
	Chitosan-MWCNTs	-	60–100	N/A	7	-	200 mg	Electrostatic interaction	N/A	The removal efficiency increases with increase of mass of both MWCNTs and Chitosan	[242]
	Nitrogen-doped magnetic carbon nanoparticles	-	-	9.31 mmol/g	8	12.82 mg/L	10 mg/500 mL	Chemical adsorption	Langmuir	Higher specific surface area and nitrogen make the nanomaterial an excellent adsorbent	[225]
Zn(II)	Oxidized MWCNTS	-	14	0.27 mmol/g	6.5–6.8	15 mg/L	5 mg/5 mL	Electrostatic interaction	Langmuir	Further research is necessary to understand the full mechanism	[199]

Table 8. *Cont.*

Adsorbate	Adsorbent	Surface Area (m^2/g)	Diameter (nm)	Q_e/RE	Experimental Conditions			Removal Mechanism	Model	Comments	Ref.
					pH	IC	AL				
	Sodium-hypochlorite-treated MWCNTs	-	<10	34.36 mg/g	-	60 mg/L	50 mg/100 mL	Electrostatic interaction	Langmuir	Zinc ion could be easily regenerated, and the adsorbent can be used for many cycles	[211]
Cu(II)	Sulfonated MWCNTs	28.7	-	43.16 mg/g	5	20 mg/L	25 mg/50 mL	Electrostatic interaction, surface complexation	D–R model	Enabling CNTs for wastewater treatment and composite formation or physical blending	[248]
	Magnetic MWCNTs	-	10–20	38.91 mg/g		30 mg/L	200 mg/1000 mL	Electrostatic interaction, physical interaction	-	Easily regenerate the Cu after removal from polluted water	[232]
	Oxidized CNT sheets	-	-	64.93 mg/g	7	200 mg/L	50 mg/25 mL	Chemical interaction	Langmuir	Considering the oxidize CNT sheets promising nanomaterial for heavy metal adsorption	[235]
	Chitosan/poly(vinyl) functionalized MWCNTs	-	5–20	11.1 mg/g	5.5	30 mg/L	0.5–2 wt%	Ion exchange	Langmuir	No loss in the adsorption capacity after four regeneration cycles	[249]
	MWCNTs modified with Chitosan	-	60–100	>95%	-	-	2000 mg	Electrostatic interaction	-	The removal efficiency increases with increase of mass of both MWCNTs and chitosan	[242]

Table 8. *Cont.*

Adsorbate	Adsorbent	Surface Area (m^2/g)	Diameter (nm)	Q_e/RE	Experimental Conditions			Removal Mechanism	Model	Comments	Ref.
					pH	IC	AL				
	Chitosan-grafted MWCNTs	-	-	24.0 mg/g	-	10mg/L	1000 mg/1000 mL	N/A	-	Effective preconcentration and solidification of heavy metals in aqueous samples	[250]
Co(II)	Poly(acrylic acid)-grafted MWCNTs	-	-	1.66×10^{-4} mol/g	6.8	1.69×10^{-4} mol/L	1.0 g/L	Surface complexation	Langmuir	Promising ability to use in water purification	[251]
	$MWCNT_S$/ iron oxide	-	-	0.18 mmol/g	6.4	4.2 mg/L	0.5 g/L	Ion exchange, surface complexation	Langmuir	Highlights the interaction between heavy metals and organic substances in wastewater	[252]
	Oxidized CNT sheets	-	-	85.74 mg/g	7	1200 mg/L	50 mg/25 mL	Chemical interaction	Langmuir	Considering the oxidized CNT sheets promising material for the removal of heavy metal ions	[235]
Ni(II)	HNO_3-treated MWCNTs	102	10–20	17.86 mg/g	6.5	20 mg/L	0.8 g/L	Ion exchange	Langmuir	Better removal efficiency toward heavy metal ions	[253]
	MWCNTs modified with Chitosan	-	60–100	90%	-	-	2000 mg	Electrostatic interaction	-	The removal efficiency increases with an increase of mass of both MWCNTs and Chitosan	[242]
	Nitrogen-doped magnetic carbon nanoparticles	-	-	8.06 mmol/g	8	12.82 mg/L	10 mg/500 mL	Chemical adsorption	Langmuir	The removal efficiency was not very good for Ni compared to Cr	[225]

Table 8. *Cont.*

Adsorbate	Adsorbent	Surface Area (m^2/g)	Diameter (nm)	Q_e/RE	Experimental Conditions			Removal Mechanism	Model	Comments	Ref.
					pH	IC	AL				
	Poly(acrylic acid) (PAA)-oxidized MWCNTs	197	-	6.615×10^{-6} mol/g	5.4	5 mg/L	0.8 g/L	Electrostatic interaction, π–π interaction	Langmuir	Effective preconcentration and solidification of Ni(II) in liquid samples	[60]
	NaClO-modified SWCNTs	-	380	47.86 mg/g	7	10–80 mg/L	50 mg/100 mL	Electrostatic interaction	Langmuir	High removal affinity to heavy metals and can be used for water treatment	[216]
	MWCNTs/ Iron oxide	-	-	9.18 mg/g	-	6 mg/L	0.75 g/L	Ion exchange	Langmuir	Promising candidate for the solidification and preconcentration of heavy metal ions as well as for radionuclides from water	[201]
	Oxidized MWCNTs	-	5.5–14	49.26 mg/g	-	10–200 mg/L	20 mg/50 mL	Electrostatic interaction	-	Greater adsorption ability than raw MWCNTs in water	[254]
	Oxidized MWCNTs	197	10–30	>80%	8	6–20 mg/L	50 mg/200 mL	Electrostatic interaction	-	Excellent material for the adsorption of metal ions.	[255]
Ni(II)	MWCNTs	40–600	40–60	6.09 mg/g	7	25 mg/L	5 g/L	Ion exchange, surface complexation, chemical interaction	-	Excellent sorption of Ni^{+2} ions with smaller equilibrium time	[256]

Table 8. *Cont.*

Adsorbate	Adsorbent	Surface Area (m^2/g)	Diameter (nm)	Q_e/RE	Experimental Conditions			Removal Mechanism	Model	Comments	Ref.
					pH	IC	AL				
U(II)	Diglycolamide-functionalized MWCNT (DGA-MWCNTs)	300–600	-	133.74 mg/g	7	-	1–10 mg	-	Langmuir	Adsorption efficiency increased with the increasing dose of adsorbent and temperature	[257]
Sr(II)	Oxidized-MWCNTs	-	-	36%	2-11	-	3 g/L	-	Diffuse layer model	Adsorption efficiency increased with increasing pH but decreased with the ionic strength	[258]
Eu (III)	Oxidized-MWCNTs	-	-	96%	2-11	-	3 g/L	-	Diffuse layer model	Higher adsorption efficiency for Eu(III) than Sr(II)	[258]

Q_e = Max adsorption capacity (mg/g); RE = Removal efficiency; IC = Initial concentration; AL = Adsorbent loading; - = Data not available

6.2. Removal of Organics

Organics due to human actions [259], animals, or plant deterioration [260] are present in water and wastewater, usually in the form of dissolved and/or suspended particulate matters [135]. Zare et al. [261] reported that the adsorption efficiencies of CNTs for organic dyes can be enhanced after the functionalization. Methylene blue and orange were effectively removed from the water matrix by using oxidized MWCNTs [262,263] as compared to other types of modified adsorbents. Duman et al. [264] successfully used a novel nanocomposite, MWCNTs/carrageenan/Fe_3O_4, for effective removal of crystal violet. New nanocomposites can also be used for CNT modification to increase the adsorption capacity of cationic dyes. Sadegh and coworkers [265] reported that the adsorption of amide black can be significantly enhanced by using MWCNT-COOH-cysteamine. The results showed a maximum adsorption capacity of 131 mg g^{-1} for MWCNT-COOH-cysteamine, while it was 90 mg g^{-1} for MWCNT-COOH [265].

The adsorption capacities of CNT composites can be reduced effectively because of competition that occurred between several types of organic contaminants present in water and wastewater at the same time [266], similarly to as described for heavy metal adsorption. However, as reported by Ali et al. [135], the initial concentration did not have any significant effect on the removal capacities of CNTs for the removal of inorganic contaminants. As a result, customization and modifications of the surface of CNTs make them significant for selective adsorption of organic contaminants. Moreover, Wang et al. showed about 95% efficiency of the CNT composite for pharmaceutical and personal care product (PPCP) removal by increasing the specific surface area and aromatic ring of CNTs [267,268]. Jahangiri-Rad et al. [269] showed an adsorption capacity of 496 mg g^{-1} by using oxidized SWCNTs with large specific surface for the removal of blue 29 dye.

Adsorption capacities and mechanisms responsible for the interaction between organic contaminants and functionalized CNTs at different experimental conditions are described in Table 9. The increase in oxygen-containing functional groups on the surface of nanotubes results in a decrease in natural organic maters (NOM), because the π–π interaction decreases due to more electrostatic repulsion [270]. The same type of results were shown in the case of higher pH [270]. Therefore, π–π interactions are responsible between the large specific surface area of functionalized CNTs and NOM for the adsorption area of CNT [271,272]. Yang et al. [208] also reported similar results, as organics may be absorbed by π–π interactions occurring between the surface of CNTs and aromatic rings of 1–naphthol.

CNTs have also been effectively used for the removal of pesticides [170]. Oxidized and as prepared MWCNTs showed excellent removal efficiency for diuron at pH $\geq$ 7.0 [273]. Oxidation of CNTs leads to the increase of their surface area, and pore size results in the higher adsorption of diuron [170]. Hamdi et al. [274] reported a reduction in uptake of chlordane and p,p′-dichlorodiphenyldichloroethylene from 78% to 23% in the roots of a lettuce crop by the addition of CNTs functionalized with amino group. The pesticides (1-pyrenebutyric, 2,4-dichlorophenoxyacetic, and diquat dibromide) were absorbed more (up to 70.6%) on semiconductor CNTs than metallic CNTs [275]. The lower density of electrons on the surface of semiconductor CNTs were found to facilitate higher adsorption [275]. On the other hand, during the batch modes, the pesticide removal was found to be limited [276]. SWCNTs and MWCNTs were used for the removal of diquat dibromide in the fixed bed system. The results were not higher than those of the batch system, but the pesticide absorbed completely in the fixed bed system by increasing the time [276].

The CNTs are also being used for nano-filtration of contaminants from aqueous solutions [162,277,278]. For adsorbents, the selectivity of nano-filters can be controlled by attaching different functional groups to the surface of CNTs [279]. Beside the hydrophobicity of CNTs, molecular dynamics simulations showed a weak interaction between water and nanotubes [280]. Hummer [281] explained that friction-free water flow was caused by the nano-scale pore size, which makes interaction energy smaller and finally lowers the interactions with water [281].

Table 9. Functionalized CNTs used for organic pollutants removal.

Adsorbent	Dye Pollutants	Surface area (m^2/g)	Q (mg/g)	Removal percentage (%)	Optimum conditions	Remarks	Ref.
Oxidized SWCNT	Basic red 46 (BR 46)	400	49.45	-	pH 9, IC = 150 mg/L, AL = 0.05 g, Contact time = 100 min, 298 K,	Exothermic process favored at lower temperature range Orderly adsorption of dye due to negative entropy	[282]
HNO3-oxidized MWCNTs	Bromothymol blue (BTB)	96.8	55	97	pH 1, IC = 30 mg/L, AL = 0.02 g, T = 293.15 K,	Endothermic process of adsorption significantly affected by pH, initial concentration, sorbent dosage, and contact time	[262]
Functionalized CNT/Mg(Al)O	Congo red	148	1250	94	pH 7, AL = 30 mg, contact time = 75 min	Strong electrostatic interactions between dye particles and functional groups associated with the surface of nanomaterial	[283]
Magnetic MWCNTs-Fe3C nanocomposite	Direct red 23	38.7	85.5	-	pH 3.7, IC = 54 mg/L, AL = 0.04 g, T = 333 K,	Spontaneous endothermic adsorption process due to positive enthalpy	[284]
SWCNT–COOH	Malachite Green	400	22.33	-	pH 7, IC = 10 mg/L, 300 K,	Adsorption significantly affected by ionic strength, initial concentration, sorbent mass, contact time, and temperature More active functional groups on SWCNT-NH2 adsorbed more dye than SWCNT-COOH	[285]
SWCNT-NH2	Malachite Green	400	29.36	-	pH 7, IC = 10 mg/L, T = 300 K,		
SWCNT–COOH	Methyl orange	400	25	-	pH 7, IC = 10 mg/L, T = 300 K,		
SWCNT-NH2	Methyl orange	400	27.15	-	pH 7, IC = 10 mg/L, T = 300 K,		
Oxidized MWCNTs	Methyl orange	165	10	-	AL = 20 mg/L, T = 313 K, stirring speed = 500 rpm	Initially, rapid adsorption was observed, but it slowed down with the time As the mixture temperature, agitation speed, and initial concentration increased, the adsorption efficiency also increased	[286]

Table 9. *Cont.*

Functionalized-CNTs loaded TiO_2	Methyl orange	-	42.85	100	pH 6.5,IC = 5 mg/L, contact time = 30 min, T = 298 K	Highly active hydroxyl and amine functional groups made TiO_2-CNT composite an effective adsorbent	[287]
Thiol-functionalized MWCNT (MWCNT-SH)	Methylene blue	400	166.67	-	pH 6,IC = 10 mg/L, AL = 20 mg, T = 298 K, Contact time = 60 min,	As the temperature and initial concentration increased, the adsorption efficiency also increased	[288]
Adsorbent	**Phenol and its derivatives pollutants**	**Q (mg/g)**	**Surface area (m2/g)**	**Removal percentage (%)**	**Optimum conditions**	**Remarks**	**Ref.**
KOH-modified MWCNTs	Bisphenol-A	0.20 mmol/g	494.48	-	pH 6, IC = 40 mg/L, contact time = 5 min, T = 298 K,	As the pH increased, the adsorption capacity decreased because of deprotonating; both the negatively charged function groups and adsorbates repel each other	[289]
HNO_3-modified MWCNTs	Bisphenol-A	0.59 mmol/g	153.79	-	pH 6, IC = 40 mg/L, contact time = 30 min, T = 298 K,		
$SOCl_2/NH_4OH$-modified CNT	Bisphenol A	69.93	94.8	-	pH 6.5, IC = 10 mg/L, AL = 0.125 g/L, T = 280 K,	Adsorption efficiency increased with the initial concentrations	[290]
NH_3-treated MWCNTs	Chlorophenols (CP)	110.3	195	-	pH 3.8, T = 298 K,	The adsorption capacity increased due to higher pores size, π–π interactions, and hydrophobicity of nanocomposite Effective nanomaterial with smaller equilibrium time	[291]
HNO_3 and $KMnO_4$-Functionalized MWCNTs	Phenol	76.92	-	88	IC = 500 mg/L, Agitation speed = 200 rpm, T = 298 K	Adsorption capacity can be greatly affected by pH and adsorbent mass	[292]
Oxidized SWNTs	*p*-Nitrophenol (PNP)	206	-	97.9	IC = 0.01 mg/mL, agitation time = 30 min T = 293 K	Open ends of nanotubes, higher surface area, and the functional groups (hydroxyl, carbonyl, and carboxyl) were responsible for higher adsorption	[293]

Table 9. *Cont.*

Nitrogen-doped carbon nanotubes (CNx)	Phenol	0.16 mmol/g	102	-	pH 7, AL = 0.6mmol/L, 298 K,	π–π interaction occurred between the functional groups and phenol; more oxidized CNTs adsorbed less phenol	[294]
MWCNT-COOH	Phenol	0.15 mmol/g	-	-	IC = 0.417 mg/L, AL = 10 mg, T = 293 K	Higher adsorption of CP than phenol resulted because of the different solubility of these contaminants	[295]
	3-Chlorophenol (CP)	0.37 mmol/g	-	95	IC = 1.25 mg/L, AL = 10 mg, T = 293 K		
Acid-functionalized MWCNT (MWCNT-COOH)	2-Nitrophenol	256.41	197.83	-	pH 5.5, IC = 45 mg/L, T = 298 K,	Excellent adsorbent due to strong interactions between 2–Nitrophenol and surface functional groups	[296]

Q = adsorption capacity, IC = Initial concentration, AL = Adsorbent loading and T = Temperature.

6.3. Removal of Microorganisms

Bacteriological contaminants, deteriorating the assimilative capacity of water bodies leading to diverse impacts on surrounding environment, are a major challenge [297]. Bacteriological contaminants are often found in surface waters, wastewaters, and respective treatment plants [145,298]. CNTs, with their diverse range of surface and functional characteristics, have a high-affinity interaction with biological contaminants. CNTs have been proven for their higher adsorption capacities, inactivation efficiencies of viral or bacterial spores, and greater antimicrobial potential than conventional sorbents because of their greater surface area [170,299,300].

Previous studies that have reported that CNTs can inactivate or remove a variety of microorganisms, including bacteria, are shown in Table 10. The inactivation of *E. coli* was observed by using SWCNTs because of its penetration into the bacterial cell wall [301]. In addition, surface-modified CNTs with different chemical groups destroy the cell wall of microorganisms more strongly than the raw and polymer-grafting CNT membranes [135]. Furthermore, the straight interaction of microbes (i.e., *E. coli*) and functionalized CNTs can cause adverse effects on the metabolisms and morphological structure of the cell wall of bacteria [135]. The penetration of CNTs into the cell wall of microorganisms is the main reason for their higher inactivation affinity [301].

CNTs functionalized with silver nanoparticles showed excellent ability to inactivate microorganisms. For example, Ihsanullah and his coworkers [302] synthesized and successfully used silver-doped CNTs for the inactivation of *E. coli* bacteria. The results proved that 100% of the bacteria were killed due to toxicity of synthesized silver doped nanomaterial [302]. In addition, many researchers reported that the diameter of nanotubes can be an important factor of concern for inactivation pathogenic microorganisms (Table 10) in water and wastewater.

The single kinetics of CNTs also reveal the CNTs' ability to eliminate pathogens in water and wastewater treatment, and microbes remain on the CNT surface based on deep filtration mechanisms [303,304]. Brady and coworkers [299] used a poly vinylidene fluoride-based SWCNT filter for excellent removal of *E. coli* bacteria at low pressure. The results show that the cells were completely captured by the filter [299]. In addition to filtrations, an excellent removal efficiency of MS2 virus was observed by filtering the sample through a controlled nano porous CNT based filter at a pressure of about 8 to 11 bar [304]. Beside the filtrations, CNTs are widely used in water and wastewater treatment as an antimicrobial agent, as described earlier. This behavior makes them a replacement for chemical disinfectants as a new method for controlling pathogens [301,305–308]. The applications of CNTs for disinfection treatment in water and wastewater avoid the materialization of unsafe disinfectant by-products like trihalomethanes, aldehydes, and haloacetic acids due to their low oxidation state and solubility in water. Therefore, it is necessary to promote the dispersibility of these compounds; a surfactant or a polymer such as sodium dodecylbenzenesulfonate, polyvinylpyrrolidone is used [309]. Due to the excellent mechanical properties on CNTs, they act as scaffolds for antimicrobial agents, such as silver nanoparticles [310,311] and antibacterial lysozyme [307,309].

Table 10. Functionalized CNTs used for disinfection.

Contaminants	Adsorbents Types	AL	IC	RE	Removal Mechanism	Comments	Ref
Escherichia coli (E. coli)	Silver-doped CNT membrane	-	1×10^6 CFU/mL	100%	-	All the bacteria were inactivated by membrane with 10% silver loadings in 60 min only	[312]
	Silver-nanoparticle-loaded CNTs	2.5 μg/mL	10^6 CFU/mL	89%	-	Effectively inactivate the pathogen from wastewater effluents, resistance toward bacterial adhesion	[313]
	Chitosan/CNT nanocomposites	2 wt%	1.5×10^8 to 5.0×10^8 CFU/mL	2.89 log reduction	Physical interaction and surface complexation	Higher antimicrobial activity at the low contact time (10 min) and low concentration (1%)	[314]
	Acidic-conditioned MWCNTs	200 μg/mL	10^6 to 10^9 CFU/mL	-	Steric obstruction	Inactivation of pathogens was due to both MWCNT functionalization and nutrition level	[315]
	1-octadecanol-functionalized MWCNTS	0.2 g/100 mL	3.5×10^7 CFU/mL	100%	Polarization	The interaction of microwaves with f-CNTs is an innovative approach that has the potential to be employed for water disinfection	[316]
Staphylococcusaureus	CNT–Ag nanohybrid	2.5 μg/mL	10^6 CFU/mL	100%	-	Effectively inactivate the pathogen from wastewater effluents, resistance toward bacterial adhesion	[313]
	Chitosan/CNTs nanocomposites	2 wt%	1.5×10^8 to 5.0×10^8 CFU/mL	4.9 log reduction	Physical interaction and surface complexation	Higher antimicrobial activity at the low contact time (10 min) and low concentration (1%)	[314]
Aspergillus flavus	Chitosan/CNTs nanocomposites	2 wt%	1.5×10^8 to 5.0×10^8 CFU/mL	5.5 log reduction	Physical interaction and surface complexation	Higher antimicrobial activity at the low contact time (10 min) and low concentration (1%)	[314]

RE = removal efficiency (%)/log reduction; AL = adsorbent loading; IC = initial concentration, mg/L; CFU/mL = colony-forming unit per milliliter.

7. Conclusions

Purifying water from assorted contaminants is challenging, and carbon nanotube-based nanocomposites can provide simple as well as effective water decontamination/disinfection. This review shows that functionalized CNTs are a new generation of pollution management materials. These materials have excellent adsorption capacities and work effectively in removing organics, inorganics, and biological species. Various sorption mechanisms include physical adsorption, electrostatic interaction, surface complexation, and chemical interactions between surface functional groups and metal ions. The effects of pH, CNT dosage, time, ionic strength, temperature, and surface charge on the adsorption of heavy metal ions on carbon nanotube surface were also discussed. Even functionalized CNTs also has antibacterial efficacy against Gram-positive and Gram-negative bacteria.

Almost all the studies show effective removal of contaminants and have been performed using deionized water, but the potential of functionalized CNT nanomaterials needs to be verified under real water conditions. In wastewater, carbonates, phosphates, and silicates can successfully compete with target metals/organics for adsorption sites in nanostructures. Other important components of source water and wastewater are natural organic materials, such as fulvic acid and humic acid, which will occupy the surface of CNTs and thus affect the adsorption of contaminants on the nanostructures. The effectiveness of CNT-based nanotechnology should be evaluated under real water conditions.

Many researchers have also focused on evaluating the adsorption–desorption capacity to make it a cost-effective adsorbent for use in wastewater treatment. However, more studies are encouraged to check the feasibility of reuse.

Author Contributions: Conceptualization, W.D. and M.M.-A.A.; resources, W.D. and H.-W.K.; writing—original draft preparation, M.M.-A.A.; writing—review and editing, H.-W.K., W.D., M.S., M.U., M.M.-A.A.; visualization, H.A.; supervision, H.-W.K. All authors have read and agreed to the published version of the manuscript.

Funding: This research received no external funding.

Institutional Review Board Statement: Not applicable.

Informed Consent Statement: Not applicable.

Data Availability Statement: Data are contained within the article.

Acknowledgments: This study was done at the Department of Environmental Science and Engineering, Tunghai University, Taiwan. The authors gratefully acknowledge the funding support by the Research Council of Texas A&M University San Antonio, and the Ministry of Science and Technology of R.O.C. (Taiwan), 107-2221-E-029-001-MY2. The authors would also like to thank Yu-Ling Wei, Chiung-Fen Chang, and Meng-Hau Sung for providing financial and analytical support to M.M.A.A. We acknowledge support of the Hamburg University of Technology (TUHH) by enabling open access publishing through funding programme Open Access Publishing.

Conflicts of Interest: The authors declare no conflict of interest.

References

1. Ali, I.; Li, J.; Peng, C.; Qasim, M.; Khan, Z.M.; Naz, I.; Sultan, M.; Rauf, M.; Iqbal, W.; Sharif, H.M.A. 3-Dimensional membrane capsules: Synthesis modulations for the remediation of environmental pollutants—A critical review. *Crit. Rev. Environ. Sci. Technol.* **2020**, 1–62. [CrossRef]
2. Usman, M.; Waseem, M.; Mani, N.; Andiego, N. Optimization of soil aquifer treatment by chemical oxidation with hydrogen peroxide addition. *Pollution* **2018**, *4*, 369–379. [CrossRef]
3. Usman, M. New Applications of Fine-Grained Iron Oxyhydroxides as Cost-Effective Arsenic Adsorbents in Water Treatment. Ph.D. Thesis, Technische Universität Hamburg, Hamburg, Germany, 2020. [CrossRef]
4. Islam, T.; Peng, C.; Ali, I.; Li, J.; Khan, Z.M.; Sultan, M.; Naz, I. Synthesis of rice husk-derived magnetic biochar through Liquefaction to adsorb anionic and cationic dyes from aqueous solutions. *Arab. J. Sci. Eng.* **2021**, *46*, 233–246. [CrossRef]
5. Khan, S.U.; Farooqi, I.H.; Usman, M.; Basheer, F. Energy efficient rapid removal of arsenic in an electrocoagulation reactor with hybrid Fe/Al electrodes: Process optimization using CCD and kinetic modeling. *Water* **2020**, *12*, 2876. [CrossRef]

6. Usman, M.; Katsoyiannis, I.; Rodrigues, J.H.; Ernst, M. Arsenate removal from drinking water using by-products from conventional iron oxyhydroxides production as adsorbents coupled with submerged microfiltration unit. *Environ. Sci. Pollut. Res.* **2020**. [CrossRef] [PubMed]
7. Amjed, M.A.; Peng, C.; Dai, M.; Chang, Q.; Ali, I.; Sultan, M.; Naz, I.; Farooq, M.Z.; Kashif, M. Recent updates on the solar-assisted biochar production and potential usage for water treatment. *Fresenius Environ. Bull.* **2020**, *29*, 5616–5632.
8. Cheng, N.; Wang, B.; Wu, P.; Lee, X.; Xing, Y.; Chen, M.; Gao, B. Adsorption of emerging contaminants from water and wastewater by modified biochar: A review. *Environ. Pollut.* **2021**, *273*, 116448. [CrossRef] [PubMed]
9. Aslam, M.M.A.; Khan, Z.M.; Sultan, M.; Niaz, Y.; Mahmood, M.H.; Shoaib, M.; Shakoor, A.; Ahmad, M. Performance evaluation of trickling filter-based wastewater treatment system utilizing cotton sticks as filter media. *Polish J. Environ. Stud.* **2017**, *26*, 1955–1962. [CrossRef]
10. Khan, Z.M.; Kanwar, R.M.A.; Farid, H.U.; Sultan, M.; Arsalan, M.; Ahmad, M.; Shakoor, A.; Aslam, M.M.A. Wastewater evaluation for multan, pakistan: Characterization and agricultural reuse. *Polish J. Environ. Stud.* **2019**, *28*, 2159–2174. [CrossRef]
11. Aslam, M.M.A.; Den, W.; Kuo, H.W. Encapsulated chitosan-modified magnetic carbon nanotubes for aqueous-phase CrVI uptake. *J. Water Process Eng.* **2021**, *40*, 101793. [CrossRef]
12. Den, W.; Wang, C.J. Removal of silica from brackish water by electrocoagulation pretreatment to prevent fouling of reverse osmosis membranes. *Sep. Purif. Technol.* **2008**, *59*, 318–325. [CrossRef]
13. Su, Y.N.; Lin, W.S.; Hou, C.H.; Den, W. Performance of integrated membrane filtration and electrodialysis processes for copper recovery from wafer polishing wastewater. *J. Water Process Eng.* **2014**, *4*, 149–158. [CrossRef]
14. Ali, I.; Peng, C.; Khan, Z.M.; Naz, I.; Sultan, M.; Ali, M.; Abbasi, I.A.; Islam, T.; Ye, T. Overview of microbes based fabricated biogenic nanoparticles for water and wastewater treatment. *J. Environ. Manag.* **2019**, *230*, 128–150. [CrossRef]
15. Ali, I.; Peng, C.; Khan, Z.M.; Naz, I.; Sultan, M. An overview of heavy metal removal from wastewater using magnetotactic bacteria. *J. Chem. Technol. Biotechnol.* **2018**, *93*, 2817–2832. [CrossRef]
16. Gupta, V.K.; Agarwal, S.; Saleh, T.A. Chromium removal by combining the magnetic properties of iron oxide with adsorption properties of carbon nanotubes. *Water Res.* **2011**, *45*, 2207–2212. [CrossRef]
17. Usman, M.; Belkasmi, A.I.; Katsoyiannis, I.A.; Ernst, M. Pre-deposited dynamic membrane adsorber formed of microscale conventional iron oxide-based adsorbents to remove arsenic from water: Application study and mathematical modeling. *J. Chem. Technol. Biotechnol.* **2021**. [CrossRef]
18. Chai, W.S.; Cheun, J.Y.; Kumar, P.S.; Mubashir, M.; Majeed, Z.; Banat, F.; Ho, S.-H.; Show, P.L. A review on conventional and novel materials towards heavy metal adsorption in wastewater treatment application. *J. Clean. Prod.* **2021**, *296*, 126589. [CrossRef]
19. Usman, M.; Zarebanadkouki, M.; Waseem, M.; Katsoyiannis, I.A.; Ernst, M. Mathematical modeling of arsenic(V) adsorption onto iron oxyhydroxides in an adsorption-submerged membrane hybrid system. *J. Hazard. Mater.* **2020**, *400*, 123221. [CrossRef] [PubMed]
20. Kyzas, G.Z.; Matis, K.A. Nanoadsorbents for pollutants removal: A review. *J. Mol. Liq.* **2015**, *203*, 159–168. [CrossRef]
21. Trujillo-Reyes, J.; Peralta-Videa, J.R.; Gardea-Torresdey, J.L. Supported and unsupported nanomaterials for water and soil remediation: Are they a useful solution for worldwide pollution? *J. Hazard. Mater.* **2014**, *280*, 487–503. [CrossRef]
22. Sharma, V.K.; McDonald, T.J.; Kim, H.; Garg, V.K. Magnetic graphene–carbon nanotube iron nanocomposites as adsorbents and antibacterial agents for water purification. *Adv. Colloid Interface Sci.* **2015**, *225*, 229–240. [CrossRef] [PubMed]
23. Qu, X.; Alvarez, P.J.J.; Li, Q. Applications of nanotechnology in water and wastewater treatment. *Water Res.* **2013**, *47*, 3931–3946. [CrossRef] [PubMed]
24. Usman, M.; Katsoyiannis, I.; Mitrakas, M.; Zouboulis, A.; Ernst, M. Performance evaluation of small sized powdered ferric hydroxide as arsenic adsorbent. *Water* **2018**, *10*, 957. [CrossRef]
25. Goh, K.; Karahan, H.E.; Wei, L.; Bae, T.-H.; Fane, A.G.; Wang, R.; Chen, Y. Carbon nanomaterials for advancing separation membranes: A strategic perspective. *Carbon N. Y.* **2016**, *109*, 694–710. [CrossRef]
26. Goh, P.S.; Ismail, A.F.; Hilal, N. Nano-enabled membranes technology: Sustainable and revolutionary solutions for membrane desalination? *Desalination* **2016**, *380*, 100–104. [CrossRef]
27. Goh, P.S.; Matsuura, T.; Ismail, A.F.; Hilal, N. Recent trends in membranes and membrane processes for desalination. *Desalination* **2016**, *391*, 43–60. [CrossRef]
28. Gupta, V.K.; Agarwal, S.; Saleh, T.A. Synthesis and characterization of alumina-coated carbon nanotubes and their application for lead removal. *J. Hazard. Mater.* **2011**, *185*, 17–23. [CrossRef]
29. Santhosh, C.; Velmurugan, V.; Jacob, G.; Jeong, S.K.; Grace, A.N.; Bhatnagar, A. Role of nanomaterials in water treatment applications: A review. *Chem. Eng. J.* **2016**, *306*, 1116–1137. [CrossRef]
30. Xu, P.; Zeng, G.M.; Huang, D.L.; Feng, C.L.; Hu, S.; Zhao, M.H.; Lai, C.; Wei, Z.; Huang, C.; Xie, G.X.; et al. Use of iron oxide nanomaterials in wastewater treatment: A review. *Sci. Total Environ.* **2012**, *424*, 1–10. [CrossRef]
31. Pendergast, M.M.; Hoek, E.M.V. A review of water treatment membrane nanotechnologies. *Energy Environ. Sci.* **2011**, *4*, 1946. [CrossRef]
32. Bethi, B.; Sonawane, S.H.; Bhanvase, B.A.; Gumfekar, S.P. Nanomaterials-based advanced oxidation processes for wastewater treatment: A review. *Chem. Eng. Process. Process Intensif.* **2016**, *109*, 178–189. [CrossRef]
33. Holmes, A.B.; Gu, F.X. Emerging nanomaterials for the application of selenium removal for wastewater treatment. *Environ. Sci. Nano* **2016**, *3*, 982–996. [CrossRef]

34. Lee, J.; Jeong, S.; Liu, Z. Progress and challenges of carbon nanotube membrane in water treatment. *Crit. Rev. Environ. Sci. Technol.* **2016**, *46*, 999–1046. [CrossRef]
35. Olivera, S.; Muralidhara, H.B.; Venkatesh, K.; Guna, V.K.; Gopalakrishna, K.; Kumar, K.Y. Potential applications of cellulose and chitosan nanoparticles/composites in wastewater treatment: A review. *Carbohydr. Polym.* **2016**, *153*, 600–618. [CrossRef]
36. Ong, C.S.; Goh, P.S.; Lau, W.J.; Misdan, N.; Ismail, A.F. Nanomaterials for biofouling and scaling mitigation of thin film composite membrane: A review. *Desalination* **2016**, *393*, 2–15. [CrossRef]
37. Stefaniuk, M.; Oleszczuk, P.; Ok, Y.S. Review on nano zerovalent iron (nZVI): From synthesis to environmental applications. *Chem. Eng. J.* **2016**, *287*, 618–632. [CrossRef]
38. Monthioux, M.; Kuznetsov, V.L. Who should be given the credit for the discovery of carbon nanotubes? *Carbon N. Y.* **2006**, *44*, 1621–1623. [CrossRef]
39. Radushkevich, L.V.; Lukyanovich, V.M. About the structure of carbon formed by thermal decomposition of carbon monoxide on iron substrate. *J. Phys. Chem.* **1952**, *26*, 88–95.
40. Oberlin, A.; Endo, M.; Koyama, T. Filamentous growth of carbon through benzene decomposition. *J. Cryst. Growth* **1976**, *32*, 335–349. [CrossRef]
41. Abrahamson, J.; Wiles, P.G.; Rhoades, B.L. Structure of carbon fibres found on carbon arc anodes. *Carbon N. Y.* **1999**, *37*, 1873–1874. [CrossRef]
42. Hirlekar, R.; Yamagar, M.; Garse, H.; Vij, M.; Kadam, V.; Vidyapeeth, B. Carbon nanotubes and its applications: A review. *Asian J. Pharm. Clin. Res.* **2009**, *2*, 17–27.
43. Tennent, H.G.; Barber, J.J.; Hoch, R. Carbon Fibrils, Method for Producing Same and Compositions Containing Same. U.S. Patent 4,663,230, 5 May 1987.
44. Bethune, D.S.; Kiang, C.H.; de Vries, M.S.; Gorman, G.; Savoy, R.; Vazquez, J.; Beyers, R. Cobalt-catalysed growth of carbon nanotubes with single-atomic-layer walls. *Nature* **1993**, *363*, 605–607. [CrossRef]
45. Iijima, S.; Ichihashi, T. Single-shell carbon nanotubes of 1-nm diameter. *Nature* **1993**, *363*, 603–605. [CrossRef]
46. Krätschmer, W.; Lamb, L.D.; Fostiropoulos, K.; Huffman, D.R. Solid C60: A new form of carbon. *Nature* **1990**, *347*, 354–358. [CrossRef]
47. Kroto, H.W.; Heath, J.R.; O'Brien, S.C.; Curl, R.F.; Smalley, R.E. C60: Buckminsterfullerene. *Nature* **1985**, *318*, 162–163. [CrossRef]
48. Liu, Z.; Sun, X.; Nakayama-Ratchford, N.; Dai, H. Supramolecular Chemistry on Water-Soluble Carbon Nanotubes for Drug Loading and Delivery. *ACS Nano* **2007**, *1*, 50–56. [CrossRef]
49. Singh, B.G.P.; Baburao, C.; Pispati, V.; Pathipati, H.; Muthy, N.; Prassana, S.R.V.; Rathode, B.G. Carbon nanotubes. A novel drug delivery system. *Int. J. Res. Pharm. Chem.* **2012**, *2*, 523–532.
50. Lam, C.; James, J.T.; McCluskey, R.; Arepalli, S.; Hunter, R.L. A review of carbon nanotube toxicity and assessment of potential occupational and environmental health risks. *Crit. Rev. Toxicol.* **2006**, *36*, 189–217. [CrossRef] [PubMed]
51. Bekyarova, E.; Ni, Y.; Malarkey, E.B.; Montana, V.; McWilliams, J.L.; Haddon, R.C.; Parpura, V. Applications of Carbon Nanotubes in Biotechnology and Biomedicine. *J. Biomed. Nanotechnol.* **2005**, *1*, 3–17. [CrossRef]
52. He, H.; Pham-Huy, L.A.; Dramou, P.; Xiao, D.; Zuo, P.; Pham-Huy, C. Carbon Nanotubes: Applications in Pharmacy and Medicine. *Biomed. Res. Int.* **2013**, *2013*, 1–12. [CrossRef]
53. Reilly, R.M. Carbon Nanotubes: Potential Benefits and Risks of Nanotechnology in Nuclear Medicine. *J. Nucl. Med.* **2007**, *48*, 1039–1042. [CrossRef] [PubMed]
54. Xie, X.; Mai, Y.; Zhou, X. Dispersion and alignment of carbon nanotubes in polymer matrix: A review. *Mater. Sci. Eng. R Rep.* **2005**, *49*, 89–112. [CrossRef]
55. Ihsanullah, A.A.; Al-Amer, A.M.; Laoui, T.; Al-Marri, M.J.; Nasser, M.S.; Khraisheh, M.; Atieh, M.A. Heavy metal removal from aqueous solution by advanced carbon nanotubes: Critical review of adsorption applications. *Sep. Purif. Technol.* **2016**, *157*, 141–161. [CrossRef]
56. Balasubramanian, K.; Burghard, M. Chemically Functionalized Carbon Nanotubes. *Small* **2005**, *1*, 180–192. [CrossRef] [PubMed]
57. Monea, B.F.; Ionete, E.I.; Spiridon, S.I.; Ion-Ebrasu, D.; Petre, E. Carbon Nanotubes and Carbon Nanotube Structures Used for Temperature Measurement. *Sensors* **2019**, *19*, 2464. [CrossRef]
58. Digge, M.; Moon, R.; Gattani, S. Application of Carbon Nanotubes in Drug Delivery: A Review. *Int. J. PharmTech Res.* **2011**, *4*, 839–847.
59. Kateb, B.; Yamamoto, V.; Alizadeh, D.; Zhang, L.; Manohara, H.M.; Bronikowski, M.J.; Badie, B. Multi-walled Carbon Nanotube (MWCNT) Synthesis, Preparation, Labeling, and Functionalization. In *Immunotherapy of Cancer*; Humana Press: Totowa, NJ, USA, 2010; pp. 307–317.
60. Liao, H.; Paratala, B.; Sitharaman, B.; Wang, Y. Applications of Carbon Nanotubes in Biomedical Studies. In *Biomedical Nanotechnology*; Humana Press: Totowa, NJ, USA, 2011; pp. 223–241.
61. Usui, Y.; Haniu, H.; Tsuruoka, S.; Saito, N. Carbon nanotubes innovate on medical technology. *Med. Chem* **2012**, *2*, 1–6. [CrossRef]
62. Yang, D.; Yang, F.; Hu, J.; Long, J.; Wang, C.; Fu, D.; Ni, Q. Hydrophilic multi-walled carbon nanotubes decorated with magnetite nanoparticles as lymphatic targeted drug delivery vehicles. *Chem. Commun.* **2009**, 4447. [CrossRef]
63. Zhang, Y.; Bai, Y.; Yan, B. Functionalized carbon nanotubes for potential medicinal applications. *Drug Discov. Today* **2010**, *15*, 428–435. [CrossRef]

64. Cassell, A.M.; Raymakers, J.A.; Kong, J.; Dai, H. Large Scale CVD Synthesis of Single-Walled Carbon Nanotubes. *J. Phys. Chem. B* **1999**, *103*, 6484–6492. [CrossRef]
65. Sinnott, S.B.; Andrews, R.; Qian, D.; Rao, A.M.; Mao, Z.; Dickey, E.C.; Derbyshire, F. Model of carbon nanotube growth through chemical vapor deposition. *Chem. Phys. Lett.* **1999**, *315*, 25–30. [CrossRef]
66. Vinciguerra, V.; Buonocore, F.; Panzera, G.; Occhipinti, L. Growth mechanisms in chemical vapour deposited carbon nanotubes. *Nanotechnology* **2003**, *14*, 655. [CrossRef]
67. Helveg, S.; López-Cartes, C.; Sehested, J.; Hansen, P.L.; Clausen, B.S.; Rostrup-Nielsen, J.R.; Abild-Pedersen, F.; Nørskov, J.K. Atomic-scale imaging of carbon nanofibre growth. *Nature* **2004**, *427*, 426–429. [CrossRef] [PubMed]
68. Maser, W.K.; Benito, A.M.; Martınez, M.T. Production of carbon nanotubes: The light approach. *Carbon N. Y.* **2002**, *40*, 1685–1695. [CrossRef]
69. Kingston, C.T.; Simard, B. Fabrication of Carbon Nanotubes. *Anal. Lett.* **2003**, *36*, 3119–3145. [CrossRef]
70. Hutchison, J.L.; Kiselev, N.A.; Krinichnaya, E.P.; Krestinin, A.V.; Loutfy, R.O.; Morawsky, A.P.; Muradyan, V.E.; Obraztsova, E.D.; Sloan, J.; Terekhov, S.V.; et al. Double-walled carbon nanotubes fabricated by a hydrogen arc discharge method. *Carbon N. Y.* **2001**, *39*, 761–770. [CrossRef]
71. Shi, Z.; Lian, Y.; Zhou, X.; Gu, Z.; Zhang, Y.; Iijima, S.; Zhou, L.; Yue, K.T.; Zhang, S. Mass-production of single-wall carbon nanotubes by arc discharge method11This work was supported by the National Natural Science Foundation of China, No. 29671030. *Carbon N. Y.* **1999**, *37*, 1449–1453. [CrossRef]
72. Sano, N.; Wang, H.; Chhowalla, M.; Alexandrou, I.; Amaratunga, G.A.J. Synthesis of carbon "onions" in water. *Nature* **2001**, *414*, 506–507. [CrossRef]
73. Li, H.; Guan, L.; Shi, Z.; Gu, Z. Direct Synthesis of High Purity Single-Walled Carbon Nanotube Fibers by Arc Discharge. *J. Phys. Chem. B* **2004**, *108*, 4573–4575. [CrossRef]
74. Imasaka, K.; Kanatake, Y.; Ohshiro, Y.; Suehiro, J.; Hara, M. Production of carbon nanoonions and nanotubes using an intermittent arc discharge in water. *Thin Solid Films* **2006**, *506–507*, 250–254. [CrossRef]
75. Sagara, T.; Kurumi, S.; Suzuki, K. Growth of linear Ni-filled carbon nanotubes by local arc discharge in liquid ethanol. *Appl. Surf. Sci.* **2014**, *292*, 39–43. [CrossRef]
76. Ben Belgacem, A.; Hinkov, I.; Yahia, S.B.; Brinza, O.; Farhat, S. Arc discharge boron nitrogen doping of carbon nanotubes. *Mater. Today Commun.* **2016**, *8*, 183–195. [CrossRef]
77. Berkmans, J.; Jagannatham, M.; Reddy, R.; Haridoss, P. Synthesis of thin bundled single walled carbon nanotubes and nanohorn hybrids by arc discharge technique in open air atmosphere. *Diam. Relat. Mater.* **2015**, *55*, 12–15. [CrossRef]
78. Su, Y.; Zhang, Y. Carbon nanomaterials synthesized by arc discharge hot plasma. *Carbon N. Y.* **2015**, *83*, 90–99. [CrossRef]
79. Guo, T.; Nikolaev, P.; Thess, A.; Colbert, D.T.; Smalley, R.E. Catalytic growth of single-walled manotubes by laser vaporization. *Chem. Phys. Lett.* **1995**, *243*, 49–54. [CrossRef]
80. Guo, T.; Nikolaev, P.; Rinzler, A.G.; Tomanek, D.; Colbert, D.T.; Smalley, R.E. Self-assembly of tubular fullerenes. *J. Phys. Chem.* **1995**, *99*, 10694–10697. [CrossRef]
81. Nagy, J.B.; Bister, G.; Fonseca, A.; Méhn, D.; Kónya, Z.; Kiricsi, I.; Horváth, Z.E.; Biró, L.P. On the Growth Mechanism of Single-Walled Carbon Nanotubes by Catalytic Carbon Vapor Deposition on Supported Metal Catalysts. *J. Nanosci. Nanotechnol.* **2004**, *4*, 326–345. [CrossRef]
82. Bandaru, P.R. Electrical Properties and Applications of Carbon Nanotube Structures. *J. Nanosci. Nanotechnol.* **2007**, *7*, 1239–1267. [CrossRef]
83. Thess, A.; Lee, R.; Nikolaev, P.; Dai, H.; Petit, P.; Robert, J.; Xu, C.; Lee, Y.H.; Kim, S.G.; Rinzler, A.G.; et al. Crystalline Ropes of Metallic Carbon Nanotubes. *Science* **1996**, *273*, 483–487. [CrossRef]
84. Journet, C.; Bernier, P. Production of carbon nanotubes. *Appl. Phys. A Mater. Sci. Process.* **1998**, *67*, 1–9. [CrossRef]
85. Ebbesen, T.W.; Hiura, H.; Fujita, J.; Ochiai, Y.; Matsui, S.; Tanigaki, K. Patterns in the bulk growth of carbon nanotubes. *Chem. Phys. Lett.* **1993**, *209*, 83–90. [CrossRef]
86. José-Yacamán, M.; Miki-Yoshida, M.; Rendón, L.; Santiesteban, J.G. Catalytic growth of carbon microtubules with fullerene structure. *Appl. Phys. Lett.* **1993**, *62*, 202–204. [CrossRef]
87. Ren, Z.F. Synthesis of Large Arrays of Well-Aligned Carbon Nanotubes on Glass. *Science* **1998**, *282*, 1105–1107. [CrossRef]
88. Oliver, J. *Global Markets and Technologies for Carbon Nanotubes: NAN024F BCC Research*; BCC Publishing: Wellesley, MA, USA, 2015.
89. Kumar, S.; Rani, R.; Dilbaghi, N.; Tankeshwar, K.; Kim, K.-H. Carbon nanotubes: A novel material for multifaceted applications in human healthcare. *Chem. Soc. Rev.* **2017**, *46*, 158–196. [CrossRef] [PubMed]
90. Ferreira, F.V.; Franceschi, W.; Menezes, B.R.C.; Biagioni, A.F.; Coutinho, A.R.; Cividanes, L.S. Synthesis, Characterization, and Applications of Carbon Nanotubes. In *Carbon-Based Nanofillers and Their Rubber Nanocomposites*; Elsevier: Amsterdam, The Netherlands, 2019; pp. 1–45.
91. Donaldson, K.; Aitken, R.; Tran, L.; Stone, V.; Duffin, R.; Forrest, G.; Alexander, A. Carbon Nanotubes: A Review of Their Properties in Relation to Pulmonary Toxicology and Workplace Safety. *Toxicol. Sci.* **2006**, *92*, 5–22. [CrossRef]
92. Ando, Y.; Zhao, X.; Sugai, T.; Kumar, M. Growing carbon nanotubes. *Mater. Today* **2004**, *7*, 22–29. [CrossRef]

93. Muataz, A.A.; Fakhrul-Razi, A.; Dayang, B.A.R.; El-Sadig, M.; Chuah, G.T.; Maan, F.A.; Sunny, I.; Faizah, Y.; Abdul Hamid, M.; Halim, M. Production of vapor growth carbon fiber (vgcf) by using cvd. In Proceedings of the 17th Symposium of Malaysian Chemical Engineers (SOMChE 2003) "Role of Chemical Engineers for Sustainability of Small Medium Industries (SMI)", Penang, Malaysia, 29–30 December 2003; pp. 596–602.
94. Cao, Z.; Sun, Z.; Guo, P.; Chen, Y. Effect of acetylene flow rate on morphology and structure of carbon nanotube thick films grown by thermal chemical vapor deposition. *Front. Mater. Sci. China* **2007**, *1*, 92–96. [CrossRef]
95. Fonseca, A.; Hernadi, K.; Piedigrosso, P.; Colomer, J.-F.; Mukhopadhyay, K.; Doome, R.; Lazarescu, S.; Biro, L.P.; Lambin, P.; Thiry, P.A.; et al. Synthesis of single- and multi-wall carbon nanotubes over supported catalysts. *Appl. Phys. A Mater. Sci. Process.* **1998**, *67*, 11–22. [CrossRef]
96. Zheng, L.X.; O'Connell, M.J.; Doorn, S.K.; Liao, X.Z.; Zhao, Y.H.; Akhadov, E.A.; Hoffbauer, M.A.; Roop, B.J.; Jia, Q.X.; Dye, R.C.; et al. Ultralong single-wall carbon nanotubes. *Nat. Mater.* **2004**, *3*, 673–676. [CrossRef]
97. Kim, N.S.; Lee, Y.T.; Park, J.; Han, J.B.; Choi, Y.S.; Choi, S.Y.; Choo, J.; Lee, G.H. Vertically Aligned Carbon Nanotubes Grown by Pyrolysis of Iron, Cobalt, and Nickel Phthalocyanines. *J. Phys. Chem. B* **2003**, *107*, 9249–9255. [CrossRef]
98. Bustero, I.; Ainara, G.; Isabel, O.; Roberto, M.; Inés, R.; Amaya, A. Control of the Properties of Carbon Nanotubes Synthesized by CVD for Application in Electrochemical Biosensors. *Microchim. Acta* **2006**, *152*, 239–247. [CrossRef]
99. Mohamed, M.M.; Ghanem, M.A.; Khairy, M.; Naguib, E.; Alotaibi, N.H. Zinc oxide incorporated carbon nanotubes or graphene oxide nanohybrids for enhanced sonophotocatalytic degradation of methylene blue dye. *Appl. Surf. Sci.* **2019**, *487*, 539–549. [CrossRef]
100. Kong, J.; Cassell, A.M.; Dai, H. Chemical vapor deposition of methane for single-walled carbon nanotubes. *Chem. Phys. Lett.* **1998**, *292*, 567–574. [CrossRef]
101. Pérez-Cabero, M.; Monzón, A.; Rodrıguez-Ramos, I.; Guerrero-Ruız, A. Syntheses of CNTs over several iron-supported catalysts: Influence of the metallic precursors. *Catal. Today* **2004**, *93–95*, 681–687. [CrossRef]
102. Zhu, S.; Su, C.-H.; Lehoczky, S.L.; Muntele, I.; Ila, D. Carbon nanotube growth on carbon fibers. *Diam. Relat. Mater.* **2003**, *12*, 1825–1828. [CrossRef]
103. Zhu, W.Z.; Miser, D.E.; Chan, W.G.; Hajaligol, M.R. Characterization of multiwalled carbon nanotubes prepared by carbon arc cathode deposit. *Mater. Chem. Phys.* **2003**, *82*, 638–647. [CrossRef]
104. Collins, P.G.; Avouris, P. Nanotubes for electronics. *Sci. Am.* **2000**, *283*, 62–69. [CrossRef]
105. Colomer, J.-F.; Stephan, C.; Lefrant, S.; Van Tendeloo, G.; Willems, I.; Kónya, Z.; Fonseca, A.; Laurent, C.; Nagy, J. Large-scale synthesis of single-wall carbon nanotubes by catalytic chemical vapor deposition (CCVD) method. *Chem. Phys. Lett.* **2000**, *317*, 83–89. [CrossRef]
106. Ebbesen, T.W.; Ajayan, P.M. Large-scale synthesis of carbon nanotubes. *Nature* **1992**, *358*, 220–222. [CrossRef]
107. Ren, Z.F.; Huang, Z.P.; Wang, D.Z.; Wen, J.G.; Xu, J.W.; Wang, J.H.; Calvet, L.E.; Chen, J.; Klemic, J.F.; Reed, M.A. Growth of a single freestanding multiwall carbon nanotube on each nanonickel dot. *Appl. Phys. Lett.* **1999**, *75*, 1086–1088. [CrossRef]
108. Yudasaka, M.; Kikuchi, R.; Matsui, T.; Ohki, Y.; Yoshimura, S.; Ota, E. Specific conditions for Ni catalyzed carbon nanotube growth by chemical vapor deposition. *Appl. Phys. Lett.* **1995**, *67*, 2477–2479. [CrossRef]
109. Yudasaka, M.; Kikuchi, R.; Ohki, Y.; Ota, E.; Yoshimura, S. Behavior of Ni in carbon nanotube nucleation. *Appl. Phys. Lett.* **1997**, *70*, 1817–1818. [CrossRef]
110. Eklund, P.C.; Pradhan, B.K.; Kim, U.J.; Xiong, Q.; Fischer, J.E.; Friedman, A.D.; Holloway, B.C.; Jordan, K.; Smith, M.W. Large-Scale Production of Single-Walled Carbon Nanotubes Using Ultrafast Pulses from a Free Electron Laser. *Nano Lett.* **2002**, *2*, 561–566. [CrossRef]
111. Maser, W.K.; Muñoz, E.; Benito, A.M.; Martınez, M.T.; de la Fuente, G.F.; Maniette, Y.; Anglaret, E.; Sauvajol, J.-L. Production of high-density single-walled nanotube material by a simple laser-ablation method. *Chem. Phys. Lett.* **1998**, *292*, 587–593. [CrossRef]
112. Bolshakov, A.P.; Uglov, S.A.; Saveliev, A.V.; Konov, V.I.; Gorbunov, A.A.; Pompe, W.; Graff, A. A novel CW laser–powder method of carbon single-wall nanotubes production. *Diam. Relat. Mater.* **2002**, *11*, 927–930. [CrossRef]
113. Scott, C.D.; Arepalli, S.; Nikolaev, P.; Smalley, R.E. Growth mechanisms for single-wall carbon nanotubes in a laser-ablation process. *Appl. Phys. A Mater. Sci. Process.* **2001**, *72*, 573–580. [CrossRef]
114. Aqel, A.; El-Nour, K.M.M.A.; Ammar, R.A.A.; Al-Warthan, A. Carbon nanotubes, science and technology part (I) structure, synthesis and characterisation. *Arab. J. Chem.* **2012**, *5*, 1–23. [CrossRef]
115. Gong, K.; Ci, L. Process for purification of carbon nanotubes. *Carbon* **2008**, *46*, 2003–2025.
116. Hou, P.; Bai, S.; Yang, Q.; Liu, C.; Cheng, H. Multi-step purification of carbon nanotubes. *Carbon N. Y.* **2002**, *40*, 81–85. [CrossRef]
117. Hajime, G.; Terumi, F.; Yoshiya, F.; Toshiyuki, O. *Method of Purifying Single Wall Carbon Nanotubes from Metal Catalyst Impurities*; JP Patent Filed & Issued; Honda Giken Kogyo Kabushiki Kaisha: Tokyo, Japan, 2002.
118. Borowiak-Palen, E.; Pichler, T.; Liu, X.; Knupfer, M.; Graff, A.; Jost, O.; Pompe, W.; Kalenczuk, R.; Fink, J. Reduced diameter distribution of single-wall carbon nanotubes by selective oxidation. *Chem. Phys. Lett.* **2002**, *363*, 567–572. [CrossRef]
119. Huang, S.; Dai, L. Plasma Etching for Purification and Controlled Opening of Aligned Carbon Nanotubes. *J. Phys. Chem. B* **2002**, *106*, 3543–3545. [CrossRef]
120. Chiang, Y.-C.; Chen, C.-H.; Chiang, Y.-C.; Chen, S.-L. Circulating inclined fluidized beds with application for desiccant dehumidification systems. *Appl. Energy* **2016**, *175*, 199–211. [CrossRef]

121. Harutyunyan, A.R.; Pradhan, B.K.; Chang, J.; Chen, G.; Eklund, P.C. Purification of Single-Wall Carbon Nanotubes by Selective Microwave Heating of Catalyst Particles. *J. Phys. Chem. B* **2002**, *106*, 8671–8675. [CrossRef]
122. Farkas, E.; Elizabeth Anderson, M.; Chen, Z.; Rinzler, A.G. Length sorting cut single wall carbon nanotubes by high performance liquid chromatography. *Chem. Phys. Lett.* **2002**, *363*, 111–116. [CrossRef]
123. Chiang, I.W.; Brinson, B.E.; Huang, A.Y.; Willis, P.A.; Bronikowski, M.J.; Margrave, J.L.; Smalley, R.E.; Hauge, R.H. Purification and Characterization of Single-Wall Carbon Nanotubes (SWNTs) Obtained from the Gas-Phase Decomposition of CO (HiPco Process). *J. Phys. Chem. B* **2001**, *105*, 8297–8301. [CrossRef]
124. Chiang, I.W.; Brinson, B.E.; Smalley, R.E.; Margrave, J.L.; Hauge, R.H. Purification and Characterization of Single-Wall Carbon Nanotubes. *J. Phys. Chem. B* **2001**, *105*, 1157–1161. [CrossRef]
125. Kajiura, H.; Tsutsui, S.; Huang, H.; Murakami, Y. High-quality single-walled carbon nanotubes from arc-produced soot. *Chem. Phys. Lett.* **2002**, *364*, 586–592. [CrossRef]
126. Moon, J.-M.; An, K.H.; Lee, Y.H.; Park, Y.S.; Bae, D.J.; Park, G.-S. High-Yield Purification Process of Singlewalled Carbon Nanotubes. *J. Phys. Chem. B* **2001**, *105*, 5677–5681. [CrossRef]
127. Doi, M.; Ikuga, Y.; Kimura, T.; Mitsuzuka, H. Laminated Sheet and Diaper and Article for Sanitary Use. JP Patent JPH10713A, Application JP8116796A, 10 May 1996.
128. Bandow, S.; Rao, A.M.; Williams, K.A.; Thess, A.; Smalley, R.E.; Eklund, P.C. Purification of Single-Wall Carbon Nanotubes by Microfiltration. *J. Phys. Chem. B* **1997**, *101*, 8839–8842. [CrossRef]
129. Sajid, M.I.; Jamshaid, U.; Jamshaid, T.; Zafar, N.; Fessi, H.; Elaissari, A. Carbon nanotubes from synthesis to in vivo biomedical applications. *Int. J. Pharm.* **2016**, *501*, 278–299. [CrossRef]
130. Hou, P.-X.; Liu, C.; Cheng, H.-M. Purification of carbon nanotubes. *Carbon N. Y.* **2008**, *46*, 2003–2025. [CrossRef]
131. Sato, Y.; Ogawa, T.; Motomiya, K.; Shinoda, K.; Jeyadevan, B.; Tohji, K.; Kasuya, A.; Nishina, Y. Purification of MWNTs Combining Wet Grinding, Hydrothermal Treatment, and Oxidation. *J. Phys. Chem. B* **2001**, *105*, 3387–3392. [CrossRef]
132. Das, R.; Abd Hamid, S.B.; Ali, M.E.; Ismail, A.F.; Annuar, M.S.M.; Ramakrishna, S. Multifunctional carbon nanotubes in water treatment: The present, past and future. *Desalination* **2014**, *354*, 160–179. [CrossRef]
133. Long, R.Q.; Yang, R.T. Carbon Nanotubes as Superior Sorbent for Dioxin Removal. *J. Am. Chem. Soc.* **2001**, *123*, 2058–2059. [CrossRef]
134. Jun, L.Y.; Mubarak, N.M.; Yee, M.J.; Yon, L.S.; Bing, C.H.; Khalid, M.; Abdullah, E.C. An overview of functionalised carbon nanomaterial for organic pollutant removal. *J. Ind. Eng. Chem.* **2018**, *67*, 175–186. [CrossRef]
135. Ali, S.; Rehman, S.A.U.; Luan, H.-Y.; Farid, M.U.; Huang, H. Challenges and opportunities in functional carbon nanotubes for membrane-based water treatment and desalination. *Sci. Total Environ.* **2019**, *646*, 1126–1139. [CrossRef]
136. Ihsanullah; Al Amer, A.M.; Laoui, T.; Abbas, A.; Al-Aqeeli, N.; Patel, F.; Khraisheh, M.; Atieh, M.A.; Hilal, N. Fabrication and antifouling behaviour of a carbon nanotube membrane. *Mater. Des.* **2016**, *89*, 549–558. [CrossRef]
137. Ihsanullah; Al-Khaldi, F.A.; Abu-Sharkh, B.; Abulkibash, A.M.; Qureshi, M.I.; Laoui, T.; Atieh, M.A. Effect of acid modification on adsorption of hexavalent chromium (Cr(VI)) from aqueous solution by activated carbon and carbon nanotubes. *Desalin. Water Treat.* **2016**, *57*, 7232–7244. [CrossRef]
138. Garzia Trulli, M.; Sardella, E.; Palumbo, F.; Palazzo, G.; Giannossa, L.C.; Mangone, A.; Comparelli, R.; Musso, S.; Favia, P. Towards highly stable aqueous dispersions of multi-walled carbon nanotubes: The effect of oxygen plasma functionalization. *J. Colloid Interface Sci.* **2017**, *491*, 255–264. [CrossRef] [PubMed]
139. Georgakilas, V.; Bourlinos, A.; Gournis, D.; Tsoufis, T.; Trapalis, C.; Mateo-Alonso, A.; Prato, M. Multipurpose Organically Modified Carbon Nanotubes: From Functionalization to Nanotube Composites. *J. Am. Chem. Soc.* **2008**, *130*, 8733–8740. [CrossRef] [PubMed]
140. Bounos, G.; Andrikopoulos, K.S.; Moschopoulou, H.; Lainioti, G.C.; Roilo, D.; Checchetto, R.; Ioannides, T.; Kallitsis, J.K.; Voyiatzis, G.A. Enhancing water vapor permeability in mixed matrix polypropylene membranes through carbon nanotubes dispersion. *J. Memb. Sci.* **2017**, *524*, 576–584. [CrossRef]
141. Oyetade, O.A.; Skelton, A.A.; Nyamori, V.O.; Jonnalagadda, S.B.; Martincigh, B.S. Experimental and DFT studies on the selective adsorption of Pb^{2+} and Zn^{2+} from aqueous solution by nitrogen-functionalized multiwalled carbon nanotubes. *Sep. Purif. Technol.* **2017**, *188*, 174–187. [CrossRef]
142. Ali, I. New Generation Adsorbents for Water Treatment. *Chem. Rev.* **2012**, *112*, 5073–5091. [CrossRef]
143. Bahgat, M.; Farghali, A.A.; El Rouby, W.M.A.; Khedr, M.H. Synthesis and modification of multi-walled carbon nano-tubes (MWCNTs) for water treatment applications. *J. Anal. Appl. Pyrolysis* **2011**, *92*, 307–313. [CrossRef]
144. Zhang, Y.; Wu, B.; Xu, H.; Liu, H.; Wang, M.; He, Y.; Pan, B. Nanomaterials-enabled water and wastewater treatment. *Nanoimpact* **2016**, *3–4*, 22–39. [CrossRef]
145. Upadhyayula, V.K.K.; Deng, S.; Mitchell, M.C.; Smith, G.B. Application of carbon nanotube technology for removal of contaminants in drinking water: A review. *Sci. Total Environ.* **2009**, *408*, 1–13. [CrossRef]
146. Rao, G.; Lu, C.; Su, F. Sorption of divalent metal ions from aqueous solution by carbon nanotubes: A review. *Sep. Purif. Technol.* **2007**, *58*, 224–231. [CrossRef]
147. Ren, X.; Chen, C.; Nagatsu, M.; Wang, X. Carbon nanotubes as adsorbents in environmental pollution management: A review. *Chem. Eng. J.* **2011**, *170*, 395–410. [CrossRef]

148. Liang, J.; Li, L.; Chen, D.; Hajagos, T.; Ren, Z.; Chou, S.-Y.; Hu, W.; Pei, Q. Intrinsically stretchable and transparent thin-film transistors based on printable silver nanowires, carbon nanotubes and an elastomeric dielectric. *Nat. Commun.* **2015**, *6*, 7647. [CrossRef]
149. Moghaddam, H.K.; Pakizeh, M. Experimental study on mercury ions removal from aqueous solution by MnO_2/CNTs nanocomposite adsorbent. *J. Ind. Eng. Chem.* **2015**, *21*, 221–229. [CrossRef]
150. Tang, W.-W.; Zeng, G.-M.; Gong, J.-L.; Liu, Y.; Wang, X.-Y.; Liu, Y.-Y.; Liu, Z.-F.; Chen, L.; Zhang, X.-R.; Tu, D.-Z. Simultaneous adsorption of atrazine and Cu (II) from wastewater by magnetic multi-walled carbon nanotube. *Chem. Eng. J.* **2012**, *211–212*, 470–478. [CrossRef]
151. Lehman, J.H.; Terrones, M.; Mansfield, E.; Hurst, K.E.; Meunier, V. Evaluating the characteristics of multiwall carbon nanotubes. *Carbon N. Y.* **2011**, *49*, 2581–2602. [CrossRef]
152. Hassellöv, M.; Readman, J.W.; Ranville, J.F.; Tiede, K. Nanoparticle analysis and characterization methodologies in environmental risk assessment of engineered nanoparticles. *Ecotoxicology* **2008**, *17*, 344–361. [CrossRef]
153. Belin, T.; Epron, F. Characterization methods of carbon nanotubes: A review. *Mater. Sci. Eng. B* **2005**, *119*, 105–118. [CrossRef]
154. Thostenson, E.T.; Ren, Z.; Chou, T.-W. Advances in the science and technology of carbon nanotubes and their composites: A review. *Compos. Sci. Technol.* **2001**, *61*, 1899–1912. [CrossRef]
155. Herrero-Latorre, C.; Álvarez-Méndez, J.; Barciela-García, J.; García-Martín, S.; Peña-Crecente, R.M. Characterization of carbon nanotubes and analytical methods for their determination in environmental and biological samples: A review. *Anal. Chim. Acta* **2015**, *853*, 77–94. [CrossRef]
156. Täschner, C.; Pácal, F.; Leonhardt, A.; Spatenka, P.; Bartsch, K.; Graff, A.; Kaltofen, R. Synthesis of aligned carbon nanotubes by DC plasma-enhanced hot filament CVD. *Surf. Coat. Technol.* **2003**, *174–175*, 81–87. [CrossRef]
157. Xiao, L.; Ha, J.W.; Wei, L.; Wang, G.; Fang, N. Determining the Full Three-Dimensional Orientation of Single Anisotropic Nanoparticles by Differential Interference Contrast Microscopy. *Angew. Chem.* **2012**, *124*, 7854–7858. [CrossRef]
158. Korneva, G.; Ye, H.; Gogotsi, Y.; Halverson, D.; Friedman, G.; Bradley, J.-C.; Kornev, K.G. Carbon Nanotubes Loaded with Magnetic Particles. *Nano Lett.* **2005**, *5*, 879–884. [CrossRef]
159. Jia, C.L.; Mi, S.B.; Faley, M.; Poppe, U.; Schubert, J.; Urban, K. Oxygen octahedron reconstruction in the $SrTiO_3$/$LaAlO_3$ heterointerfaces investigated using aberration-corrected ultrahigh-resolution transmission electron microscopy. *Phys. Rev. B* **2009**, *79*, 081405. [CrossRef]
160. Gao, C.; Stading, M.; Wellner, N.; Parker, M.L.; Noel, T.R.; Mills, E.N.C.; Belton, P.S. Plasticization of a Protein-Based Film by Glycerol: A Spectroscopic, Mechanical, and Thermal Study. *J. Agric. Food Chem.* **2006**, *54*, 4611–4616. [CrossRef] [PubMed]
161. Sun, Y.-P.; Fu, K.; Lin, Y.; Huang, W. Functionalized Carbon Nanotubes: Properties and Applications. *Acc. Chem. Res.* **2002**, *35*, 1096–1104. [CrossRef] [PubMed]
162. Jin, S.; Fallgren, P.H.; Morris, J.M.; Chen, Q. Removal of bacteria and viruses from waters using layered double hydroxide nanocomposites. *Sci. Technol. Adv. Mater.* **2007**, *8*, 67–70. [CrossRef]
163. Huang, J.; Cao, Y.; Qin, B.; Zhong, G.; Zhang, J.; Yu, H.; Wang, H.; Peng, F. Highly efficient and acid-corrosion resistant nitrogen doped magnetic carbon nanotubes for the hexavalent chromium removal with subsequent reutilization. *Chem. Eng. J.* **2019**, *361*, 547–558. [CrossRef]
164. Correa-Duarte, M.A.; Grzelczak, M.; Salgueiriño-Maceira, V.; Giersig, M.; Liz-Marzán, L.M.; Farle, M.; Sierazdki, K.; Diaz, R. Alignment of Carbon Nanotubes under Low Magnetic Fields through Attachment of Magnetic Nanoparticles. *J. Phys. Chem. B* **2005**, *109*, 19060–19063. [CrossRef]
165. Rinzler, A.G.; Liu, J.; Dai, H.; Nikolaev, P.; Huffman, C.B.; Rodríguez-Macías, F.J.; Boul, P.J.; Lu, A.H.; Heymann, D.; Colbert, D.T.; et al. Large-scale purification of single-wall carbon nanotubes: Process, product, and characterization. *Appl. Phys. A Mater. Sci. Process.* **1998**, *67*, 29–37. [CrossRef]
166. Gommes, C.; Blacher, S.; Masenelli-Varlot, K.; Bossuot, C.; McRae, E.; Fonseca, A.; Nagy, J.-B.; Pirard, J.-P. Image analysis characterization of multi-walled carbon nanotubes. *Carbon N. Y.* **2003**, *41*, 2561–2572. [CrossRef]
167. Jimeno, A.; Goyanes, S.; Eceiza, A.; Kortaberria, G.; Mondragon, I.; Corcuera, M.A. Effects of Amine Molecular Structure on Carbon Nanotubes Functionalization. *J. Nanosci. Nanotechnol.* **2009**, *9*, 6222–6227. [CrossRef]
168. Chai, S.-P.; Zein, S.H.S.; Mohamed, A.R. The effect of reduction temperature on Co-Mo/Al2O3 catalysts for carbon nanotubes formation. *Appl. Catal. A Gen.* **2007**, *326*, 173–179. [CrossRef]
169. Kiang, C.-H.; Endo, M.; Ajayan, P.M.; Dresselhaus, G.; Dresselhaus, M.S. Size Effects in Carbon Nanotubes. *Phys. Rev. Lett.* **1998**, *81*, 1869–1872. [CrossRef]
170. Sarkar, C.; Chowdhuri, A.R.; Kumar, A.; Laha, D.; Garai, S.; Chakraborty, J.; Sahu, S.K. One pot synthesis of carbon dots decorated carboxymethyl cellulose- hydroxyapatite nanocomposite for drug delivery, tissue engineering and Fe^{3+} ion sensing. *Carbohydr. Polym.* **2018**, *181*, 710–718. [CrossRef]
171. Wepasnick, K.A.; Smith, B.A.; Bitter, J.L.; Howard Fairbrother, D. Chemical and structural characterization of carbon nanotube surfaces. *Anal. Bioanal. Chem.* **2010**, *396*, 1003–1014. [CrossRef]
172. Datsyuk, V.; Kalyva, M.; Papagelis, K.; Parthenios, J.; Tasis, D.; Siokou, A.; Kallitsis, I.; Galiotis, C. Chemical oxidation of multiwalled carbon nanotubes. *Carbon N. Y.* **2008**, *46*, 833–840. [CrossRef]
173. Liu, M.; Cowley, J.M. Structures of carbon nanotubes studied by HRTEM and nanodiffraction. *Ultramicroscopy* **1994**, *53*, 333–342. [CrossRef]

174. Cao, A.; Zhang, X.; Xu, C.; Wei, B.; Wu, D. Tandem structure of aligned carbon nanotubes on Au and its solar thermal absorption. *Sol. Energy Mater. Sol. Cells* **2002**, *70*, 481–486. [CrossRef]
175. Droppa, R.; Hammer, P.; Carvalho, A.C.; dos Santos, M.; Alvarez, F. Incorporation of nitrogen in carbon nanotubes. *J. Non-Cryst. Solids* **2002**, *299–302*, 874–879. [CrossRef]
176. Chong, C.T.; Tan, W.H.; Lee, S.L.; Chong, W.W.F.; Lam, S.S.; Valera-Medina, A. Morphology and growth of carbon nanotubes catalytically synthesised by premixed hydrocarbon-rich flames. *Mater. Chem. Phys.* **2017**, *197*, 246–255. [CrossRef]
177. Hammer, P.; Victoria, N.M.; Alvarez, F. Effects of increasing nitrogen concentration on the structure of carbon nitride films deposited by ion beam assisted deposition. *J. Vac. Sci. Technol. A Vac. Surfaces Film.* **2000**, *18*, 2277. [CrossRef]
178. Pham-Huu, C.; Keller, N.; Roddatis, V.V.; Mestl, G.; Schlögl, R.; Ledoux, M.J. Large scale synthesis of carbon nanofibers by catalytic decomposition of ethane on nickel nanoclusters decorating carbon nanotubes. *Phys. Chem. Chem. Phys.* **2002**, *4*, 514–521. [CrossRef]
179. Lee, Y.S.; Cho, T.H.; Lee, B.K.; Rho, J.S.; An, K.H.; Lee, Y.H. Surface properties of fluorinated single-walled carbon nanotubes. *J. Fluor. Chem.* **2003**, *120*, 99–104. [CrossRef]
180. Cao, A.; Xu, C.; Liang, J.; Wu, D.; Wei, B. X-ray diffraction characterization on the alignment degree of carbon nanotubes. *Chem. Phys. Lett.* **2001**, *344*, 13–17. [CrossRef]
181. Rols, S.; Almairac, R.; Henrard, L.; Anglaret, E.; Sauvajol, J.-L. Diffraction by finite-size crystalline bundles of single wall nanotubes. *Eur. Phys. J. B* **1999**, *10*, 263–270. [CrossRef]
182. Kuzmany, H.; Plank, W.; Hulman, M.; Kramberger, C.; Grüneis, A.; Pichler, T.; Peterlik, H.; Kataura, H.; Achiba, Y. Determination of SWCNT diameters from the Raman response of the radial breathing mode. *Eur. Phys. J. B* **2001**, *22*, 307–320. [CrossRef]
183. Santos, T.C.; dos Gates, R.S.; de Tinôco, I.F.F.; Zolnier, S.; da Baêta, F.C. Behavior of Japanese quail in different air velocities and air temperatures. *Pesqui. Agropecuária Bras.* **2017**, *52*, 344–354. [CrossRef]
184. Cividanes, L.S.; Brunelli, D.D.; Antunes, E.F.; Corat, E.J.; Sakane, K.K.; Thim, G.P. Cure study of epoxy resin reinforced with multiwalled carbon nanotubes by Raman and luminescence spectroscopy. *J. Appl. Polym. Sci.* **2013**, *127*, 544–553. [CrossRef]
185. Puangjan, A.; Chaiyasith, S.; Taweeporngitgul, W.; Keawtep, J. Application of functionalized multi-walled carbon nanotubes supporting cuprous oxide and silver oxide composite catalyst on copper substrate for simultaneous detection of vitamin B2, vitamin B6 and ascorbic acid. *Mater. Sci. Eng. C* **2017**, *76*, 383–397. [CrossRef]
186. Ferreira, F.V.; Francisco, W.; Menezes, B.R.C.; Brito, F.S.; Coutinho, A.S.; Cividanes, L.S.; Coutinho, A.R.; Thim, G.P. Correlation of surface treatment, dispersion and mechanical properties of HDPE/CNT nanocomposites. *Appl. Surf. Sci.* **2016**, *389*, 921–929. [CrossRef]
187. Silambarasan, D.; Surya, V.J.; Iyakutti, K.; Asokan, K.; Vasu, V.; Kawazoe, Y. Gamma (γ)-ray irradiated multi-walled carbon nanotubes (MWCNTs) for hydrogen storage. *Appl. Surf. Sci.* **2017**, *418*, 49–55. [CrossRef]
188. Arepalli, S.; Nikolaev, P.; Gorelik, O.; Hadjiev, V.G.; Holmes, W.; Files, B.; Yowell, L. Protocol for the characterization of single-wall carbon nanotube material quality. *Carbon N. Y.* **2004**, *42*, 1783–1791. [CrossRef]
189. Alvarez, W.E.; Kitiyanan, B.; Borgna, A.; Resasco, D.E. Synergism of Co and Mo in the catalytic production of single-wall carbon nanotubes by decomposition of CO. *Carbon N. Y.* **2001**, *39*, 547–558. [CrossRef]
190. Bahr, J.L.; Yang, J.; Kosynkin, D.V.; Bronikowski, M.J.; Smalley, R.E.; Tour, J.M. Functionalization of Carbon Nanotubes by Electrochemical Reduction of Aryl Diazonium Salts: A Bucky Paper Electrode. *J. Am. Chem. Soc.* **2001**, *123*, 6536–6542. [CrossRef]
191. Liu, W.-W.; Aziz, A.; Chai, S.-P.; Mohamed, A.R.; Tye, C.-T. Preparation of iron oxide nanoparticles supported on magnesium oxide for producing high-quality single-walled carbon nanotubes. *New Carbon Mater.* **2011**, *26*, 255–261. [CrossRef]
192. Anoshkin, I.V.; Nefedova, I.I.; Lioubtchenko, D.V.; Nefedov, I.S.; Räisänen, A.V. Single walled carbon nanotube quantification method employing the Raman signal intensity. *Carbon N. Y.* **2017**, *116*, 547–552. [CrossRef]
193. Xue, Y.; Zheng, S.; Sun, Z.; Zhang, Y.; Jin, W. Alkaline electrochemical advanced oxidation process for chromium oxidation at graphitized multi-walled carbon nanotubes. *Chemosphere* **2017**, *183*, 156–163. [CrossRef]
194. Faraji, S.; Yildiz, O.; Rost, C.; Stano, K.; Farahbakhsh, N.; Zhu, Y.; Bradford, P.D. Radial growth of multi-walled carbon nanotubes in aligned sheets through cyclic carbon deposition and graphitization. *Carbon N. Y.* **2017**, *111*, 411–418. [CrossRef]
195. Pillay, K.; Cukrowska, E.M.; Coville, N.J. Multi-walled carbon nanotubes as adsorbents for the removal of parts per billion levels of hexavalent chromium from aqueous solution. *J. Hazard. Mater.* **2009**, *166*, 1067–1075. [CrossRef]
196. Yu, F.; Ma, J.; Wang, J.; Zhang, M.; Zheng, J. Magnetic iron oxide nanoparticles functionalized multi-walled carbon nanotubes for toluene, ethylbenzene and xylene removal from aqueous solution. *Chemosphere* **2016**, *146*, 162–172. [CrossRef]
197. Usman Farid, M.; Luan, H.-Y.; Wang, Y.; Huang, H.; An, A.K.; Jalil Khan, R. Increased adsorption of aqueous zinc species by Ar/O 2 plasma-treated carbon nanotubes immobilized in hollow-fiber ultrafiltration membrane. *Chem. Eng. J.* **2017**, *325*, 239–248. [CrossRef]
198. Agnihotri, S.; Mota, J.P.B.; Rostam-Abadi, M.; Rood, M.J. Theoretical and Experimental Investigation of Morphology and Temperature Effects on Adsorption of Organic Vapors in Single-Walled Carbon Nanotubes. *J. Phys. Chem. B* **2006**, *110*, 7640–7647. [CrossRef]
199. Cho, H.-H.; Wepasnick, K.; Smith, B.A.; Bangash, F.K.; Fairbrother, D.H.; Ball, W.P. Sorption of Aqueous Zn[II] and Cd[II] by Multiwall Carbon Nanotubes: The Relative Roles of Oxygen-Containing Functional Groups and Graphenic Carbon. *Langmuir* **2010**, *26*, 967–981. [CrossRef]

200. Yu, X.-Y.; Luo, T.; Zhang, Y.-X.; Jia, Y.; Zhu, B.-J.; Fu, X.-C.; Liu, J.-H.; Huang, X.-J. Adsorption of Lead(II) on O_2-Plasma-Oxidized Multiwalled Carbon Nanotubes: Thermodynamics, Kinetics, and Desorption. *ACS Appl. Mater. Interfaces* **2011**, *3*, 2585–2593. [CrossRef]
201. Addo Ntim, S.; Mitra, S. Removal of Trace Arsenic To Meet Drinking Water Standards Using Iron Oxide Coated Multiwall Carbon Nanotubes. *J. Chem. Eng. Data* **2011**, *56*, 2077–2083. [CrossRef] [PubMed]
202. Chen, C.; Hu, J.; Shao, D.; Li, J.; Wang, X. Adsorption behavior of multiwall carbon nanotube/iron oxide magnetic composites for Ni(II) and Sr(II). *J. Hazard. Mater.* **2009**, *164*, 923–928. [CrossRef] [PubMed]
203. Daneshvar Tarigh, G.; Shemirani, F. Magnetic multi-wall carbon nanotube nanocomposite as an adsorbent for preconcentration and determination of lead (II) and manganese (II) in various matrices. *Talanta* **2013**, *115*, 744–750. [CrossRef]
204. Zhao, X.; Jia, Q.; Song, N.; Zhou, W.; Li, Y. Adsorption of Pb(II) from an Aqueous Solution by Titanium Dioxide/Carbon Nanotube Nanocomposites: Kinetics, Thermodynamics, and Isotherms. *J. Chem. Eng. Data* **2010**, *55*, 4428–4433. [CrossRef]
205. Gupta, A.; Vidyarthi, S.R.; Sankararamakrishnan, N. Enhanced sorption of mercury from compact fluorescent bulbs and contaminated water streams using functionalized multiwalled carbon nanotubes. *J. Hazard. Mater.* **2014**, *274*, 132–144. [CrossRef]
206. Gupta, V.K.; Moradi, O.; Tyagi, I.; Agarwal, S.; Sadegh, H.; Shahryari-Ghoshekandi, R.; Makhlouf, A.S.H.; Goodarzi, M.; Garshasbi, A. Study on the removal of heavy metal ions from industry waste by carbon nanotubes: Effect of the surface modification: A review. *Crit. Rev. Environ. Sci. Technol.* **2016**, *46*, 93–118. [CrossRef]
207. Hu, J.; Zhao, D.; Wang, X. Removal of Pb(II) and Cu(II) from aqueous solution using multiwalled carbon nanotubes/iron oxide magnetic composites. *Water Sci. Technol.* **2011**, *63*, 917–923. [CrossRef]
208. Yang, S.; Guo, Z.; Sheng, G.; Wang, X. Investigation of the sequestration mechanisms of Cd(II) and 1-naphthol on discharged multi-walled carbon nanotubes in aqueous environment. *Sci. Total Environ.* **2012**, *420*, 214–221. [CrossRef]
209. Vuković, G.D.; Marinković, A.D.; Čolić, M.; Ristić, M.Đ.; Aleksić, R.; Perić-Grujić, A.A.; Uskoković, P.S. Removal of cadmium from aqueous solutions by oxidized and ethylenediamine-functionalized multi-walled carbon nanotubes. *Chem. Eng. J.* **2010**, *157*, 238–248. [CrossRef]
210. Stafiej, A.; Pyrzynska, K. Solid phase extraction of metal ions using carbon nanotubes. *Microchem. J.* **2008**, *89*, 29–33. [CrossRef]
211. Lu, C.; Chiu, H. Adsorption of zinc(II) from water with purified carbon nanotubes. *Chem. Eng. Sci.* **2006**, *61*, 1138–1145. [CrossRef]
212. Weng, C.-H.; Huang, C.P. Adsorption characteristics of Zn(II) from dilute aqueous solution by fly ash. *Colloids Surf. A Physicochem. Eng. Asp.* **2004**, *247*, 137–143. [CrossRef]
213. Boehm, H. Surface oxides on carbon and their analysis: A critical assessment. *Carbon N. Y.* **2002**, *40*, 145–149. [CrossRef]
214. Li, J.; Chen, S.; Sheng, G.; Hu, J.; Tan, X.; Wang, X. Effect of surfactants on Pb(II) adsorption from aqueous solutions using oxidized multiwall carbon nanotubes. *Chem. Eng. J.* **2011**, *166*, 551–558. [CrossRef]
215. Atieh, M.A.; Bakather, O.Y.; Tawabini, B.S.; Bukhari, A.A.; Khaled, M.; Alharthi, M.; Fettouhi, M.; Abuilaiwi, F.A. Removal of Chromium (III) from Water by Using Modified and Nonmodified Carbon Nanotubes. *J. Nanomater.* **2010**, *2010*, 1–9. [CrossRef]
216. Lu, C.; Liu, C.; Rao, G.P. Comparisons of sorbent cost for the removal of Ni2+ from aqueous solution by carbon nanotubes and granular activated carbon. *J. Hazard. Mater.* **2008**, *151*, 239–246. [CrossRef]
217. Ali, I. Microwave assisted economic synthesis of multi walled carbon nanotubes for arsenic species removal in water: Batch and column operations. *J. Mol. Liq.* **2018**, *271*, 677–685. [CrossRef]
218. Alijani, H.; Shariatinia, Z. Effective aqueous arsenic removal using zero valent iron doped MWCNT synthesized by in situ CVD method using natural α-Fe_2O_3 as a precursor. *Chemosphere* **2017**, *171*, 502–511. [CrossRef]
219. Sankararamakrishnan, N.; Chauhan, D.; Dwivedi, J. Synthesis of functionalized carbon nanotubes by floating catalytic chemical vapor deposition method and their sorption behavior toward arsenic. *Chem. Eng. J.* **2016**, *284*, 599–608. [CrossRef]
220. Ma, M.-D.; Wu, H.; Deng, Z.-Y.; Zhao, X. Arsenic removal from water by nanometer iron oxide coated single-wall carbon nanotubes. *J. Mol. Liq.* **2018**, *259*, 369–375. [CrossRef]
221. Peng, H.; Zhang, N.; He, M.; Chen, B.; Hu, B. Simultaneous speciation analysis of inorganic arsenic, chromium and selenium in environmental waters by 3-(2-aminoethylamino) propyltrimethoxysilane modified multi-wall carbon nanotubes packed microcolumn solid phase extraction and ICP-MS. *Talanta* **2015**, *131*, 266–272. [CrossRef]
222. Veličković, Z.; Vuković, G.D.; Marinković, A.D.; Moldovan, M.-S.; Perić-Grujić, A.A.; Uskoković, P.S.; Ristić, M.Đ. Adsorption of arsenate on iron(III) oxide coated ethylenediamine functionalized multiwall carbon nanotubes. *Chem. Eng. J.* **2012**, *181–182*, 174–181. [CrossRef]
223. Addo Ntim, S.; Mitra, S. Adsorption of arsenic on multiwall carbon nanotube–zirconia nanohybrid for potential drinking water purification. *J. Colloid Interface Sci.* **2012**, *375*, 154–159. [CrossRef]
224. De Marques Neto, J.O.; Bellato, C.R.; de Silva, D.C. Iron oxide/carbon nanotubes/chitosan magnetic composite film for chromium species removal. *Chemosphere* **2019**, *218*, 391–401. [CrossRef]
225. Shin, K.-Y.; Hong, J.-Y.; Jang, J. Heavy metal ion adsorption behavior in nitrogen-doped magnetic carbon nanoparticles: Isotherms and kinetic study. *J. Hazard. Mater.* **2011**, *190*, 36–44. [CrossRef]
226. Huang, Y.; Lee, X.; Macazo, F.C.; Grattieri, M.; Cai, R.; Minteer, S.D. Fast and efficient removal of chromium (VI) anionic species by a reusable chitosan-modified multi-walled carbon nanotube composite. *Chem. Eng. J.* **2018**, *339*, 259–267. [CrossRef]
227. Lu, W.; Li, J.; Sheng, Y.; Zhang, X.; You, J.; Chen, L. One-pot synthesis of magnetic iron oxide nanoparticle-multiwalled carbon nanotube composites for enhanced removal of Cr(VI) from aqueous solution. *J. Colloid Interface Sci.* **2017**, *505*, 1134–1146. [CrossRef]

228. Salam, M.A. Preparation and characterization of chitin/magnetite/multiwalled carbon nanotubes magnetic nanocomposite for toxic hexavalent chromium removal from solution. *J. Mol. Liq.* **2017**, *233*, 197–202. [CrossRef]
229. Huang, Z.; Wang, X.; Yang, D. Adsorption of Cr(VI) in wastewater using magnetic multi-wall carbon nanotubes. *Water Sci. Eng.* **2015**, *8*, 226–232. [CrossRef]
230. Di, Z.-C.; Ding, J.; Peng, X.-J.; Li, Y.-H.; Luan, Z.-K.; Liang, J. Chromium adsorption by aligned carbon nanotubes supported ceria nanoparticles. *Chemosphere* **2006**, *62*, 861–865. [CrossRef] [PubMed]
231. Zhang, C.; Sui, J.; Li, J.; Tang, Y.; Cai, W. Efficient removal of heavy metal ions by thiol-functionalized superparamagnetic carbon nanotubes. *Chem. Eng. J.* **2012**, *210*, 45–52. [CrossRef]
232. Wang, G.; Gao, Z.; Tang, S.; Chen, C.; Duan, F.; Zhao, S.; Lin, S.; Feng, Y.; Zhou, L.; Qin, Y. Microwave Absorption Properties of Carbon Nanocoils Coated with Highly Controlled Magnetic Materials by Atomic Layer Deposition. *ACS Nano* **2012**, *6*, 11009–11017. [CrossRef] [PubMed]
233. Ji, L.; Zhou, L.; Bai, X.; Shao, Y.; Zhao, G.; Qu, Y.; Wang, C.; Li, Y. Facile synthesis of multiwall carbon nanotubes/iron oxides for removal of tetrabromobisphenol A and Pb(ii). *J. Mater. Chem.* **2012**, *22*, 15853. [CrossRef]
234. Yang, L.; Jiang, S.; Zhao, Y.; Zhu, L.; Chen, S.; Wang, X.; Wu, Q.; Ma, J.; Ma, Y.; Hu, Z. Boron-Doped Carbon Nanotubes as Metal-Free Electrocatalysts for the Oxygen Reduction Reaction. *Angew. Chem. Int. Ed.* **2011**, *50*, 7132–7135. [CrossRef] [PubMed]
235. Tofighy, M.A.; Mohammadi, T. Adsorption of divalent heavy metal ions from water using carbon nanotube sheets. *J. Hazard. Mater.* **2011**, *185*, 140–147. [CrossRef]
236. Ren, X.; Shao, D.; Zhao, G.; Sheng, G.; Hu, J.; Yang, S.; Wang, X. Plasma Induced Multiwalled Carbon Nanotube Grafted with 2-Vinylpyridine for Preconcentration of Pb(II) from Aqueous Solutions. *Plasma Process. Polym.* **2011**, *8*, 589–598. [CrossRef]
237. Xu, D.; Wang, Z. Role of multi-wall carbon nanotube network in composites to crystallization of isotactic polypropylene matrix. *Polymer* **2008**, *49*, 330–338. [CrossRef]
238. Wang, S.; Gong, W.; Liu, X.; Yao, Y.; Gao, B.; Yue, Q. Removal of lead(II) from aqueous solution by adsorption onto manganese oxide-coated carbon nanotubes. *Sep. Purif. Technol.* **2007**, *58*, 17–23. [CrossRef]
239. Wang, H.J.; Zhou, A.L.; Peng, F.; Yu, H.; Chen, L.F. Adsorption characteristic of acidified carbon nanotubes for heavy metal Pb(II) in aqueous solution. *Mater. Sci. Eng. A* **2007**, *466*, 201–206. [CrossRef]
240. Liang, J.; Liu, J.; Yuan, X.; Dong, H.; Zeng, G.; Wu, H.; Wang, H.; Liu, J.; Hua, S.; Zhang, S.; et al. Facile synthesis of alumina-decorated multi-walled carbon nanotubes for simultaneous adsorption of cadmium ion and trichloroethylene. *Chem. Eng. J.* **2015**, *273*, 101–110. [CrossRef]
241. Al-Khaldi, F.A.; Abusharkh, B.; Khaled, M.; Atieh, M.A.; Nasser, M.S.; Saleh, T.A.; Agarwal, S.; Tyagi, I.; Gupta, V.K. Adsorptive removal of cadmium(II) ions from liquid phase using acid modified carbon-based adsorbents. *J. Mol. Liq.* **2015**, *204*, 255–263. [CrossRef]
242. Salam, M.A.; Makki, M.S.I.; Abdelaal, M.Y.A. Preparation and characterization of multi-walled carbon nanotubes/chitosan nanocomposite and its application for the removal of heavy metals from aqueous solution. *J. Alloys Compd.* **2011**, *509*, 2582–2587. [CrossRef]
243. Bandaru, N.M.; Reta, N.; Dalal, H.; Ellis, A.V.; Shapter, J.; Voelcker, N.H. Enhanced adsorption of mercury ions on thiol derivatized single wall carbon nanotubes. *J. Hazard. Mater.* **2013**, *261*, 534–541. [CrossRef]
244. Hadavifar, M.; Bahramifar, N.; Younesi, H.; Li, Q. Adsorption of mercury ions from synthetic and real wastewater aqueous solution by functionalized multi-walled carbon nanotube with both amino and thiolated groups. *Chem. Eng. J.* **2014**, *237*, 217–228. [CrossRef]
245. Pillay, K.; Cukrowska, E.M.; Coville, N.J. Improved uptake of mercury by sulphur-containing carbon nanotubes. *Microchem. J.* **2013**, *108*, 124–130. [CrossRef]
246. El-Sheikh, A.H.; Al-Degs, Y.S.; Al-As'ad, R.M.; Sweileh, J.A. Effect of oxidation and geometrical dimensions of carbon nanotubes on Hg(II) sorption and preconcentration from real waters. *Desalination* **2011**, *270*, 214–220. [CrossRef]
247. Mubarak, N.M.; Alicia, R.F.; Abdullah, E.C.; Sahu, J.N.; Haslija, A.B.A.; Tan, J. Statistical optimization and kinetic studies on removal of Zn2+ using functionalized carbon nanotubes and magnetic biochar. *J. Environ. Chem. Eng.* **2013**, *1*, 486–495. [CrossRef]
248. Ge, Y.; Li, Z.; Xiao, D.; Xiong, P.; Ye, N. Sulfonated multi-walled carbon nanotubes for the removal of copper (II) from aqueous solutions. *J. Ind. Eng. Chem.* **2014**, *20*, 1765–1771. [CrossRef]
249. Salehi, E.; Madaeni, S.S.; Rajabi, L.; Vatanpour, V.; Derakhshan, A.A.; Zinadini, S.; Ghorabi, S.; Ahmadi Monfared, H. Novel chitosan/poly(vinyl) alcohol thin adsorptive membranes modified with amino functionalized multi-walled carbon nanotubes for Cu(II) removal from water: Preparation, characterization, adsorption kinetics and thermodynamics. *Sep. Purif. Technol.* **2012**, *89*, 309–319. [CrossRef]
250. Shao, D.; Hu, J.; Chen, C.; Sheng, G.; Ren, X.; Wang, X. Polyaniline Multiwalled Carbon Nanotube Magnetic Composite Prepared by Plasma-Induced Graft Technique and Its Application for Removal of Aniline and Phenol. *J. Phys. Chem. C* **2010**, *114*, 21524–21530. [CrossRef]
251. Chen, H.; Li, J.; Shao, D.; Ren, X.; Wang, X. Poly(acrylic acid) grafted multiwall carbon nanotubes by plasma techniques for Co(II) removal from aqueous solution. *Chem. Eng. J.* **2012**, *210*, 475–481. [CrossRef]
252. Wang, Q.; Li, J.; Chen, C.; Ren, X.; Hu, J.; Wang, X. Removal of cobalt from aqueous solution by magnetic multiwalled carbon nanotube/iron oxide composites. *Chem. Eng. J.* **2011**, *174*, 126–133. [CrossRef]

253. Mobasherpour, I.; Salahi, E.; Ebrahimi, M. Removal of divalent nickel cations from aqueous solution by multi-walled carbon nano tubes: Equilibrium and kinetic processes. *Res. Chem. Intermed.* **2012**, *38*, 2205–2222. [CrossRef]
254. Kandah, M.I.; Meunier, J.-L. Removal of nickel ions from water by multi-walled carbon nanotubes. *J. Hazard. Mater.* **2007**, *146*, 283–288. [CrossRef]
255. Chen, C.; Wang, X. Adsorption of Ni(II) from Aqueous Solution Using Oxidized Multiwall Carbon Nanotubes. *Ind. Eng. Chem. Res.* **2006**, *45*, 9144–9149. [CrossRef]
256. Abdel-Ghani, N.T.; El-Chaghaby, G.A.; Helal, F.S. Individual and competitive adsorption of phenol and nickel onto multiwalled carbon nanotubes. *J. Adv. Res.* **2015**, *6*, 405–415. [CrossRef]
257. Deb, A.K.S.; Ilaiyaraja, P.; Ponraju, D.; Venkatraman, B. Diglycolamide functionalized multi-walled carbon nanotubes for removal of uranium from aqueous solution by adsorption. *J. Radioanal. Nucl. Chem.* **2012**, *291*, 877–883. [CrossRef]
258. Chen, C.; Hu, J.; Xu, D.; Tan, X.; Meng, Y.; Wang, X. Surface complexation modeling of Sr(II) and Eu(III) adsorption onto oxidized multiwall carbon nanotubes. *J. Colloid Interface Sci.* **2008**, *323*, 33–41. [CrossRef]
259. Tousova, Z.; Oswald, P.; Slobodnik, J.; Blaha, L.; Muz, M.; Hu, M.; Brack, W.; Krauss, M.; Di Paolo, C.; Tarcai, Z.; et al. European demonstration program on the effect-based and chemical identification and monitoring of organic pollutants in European surface waters. *Sci. Total Environ.* **2017**, *601–602*, 1849–1868. [CrossRef]
260. Sillanpää, M. *Natural Organic Matter in Water*, 1st ed.; Elsevier: Amsterdam, The Netherlands, 2015; ISBN 9780128015032.
261. Zare, K.; Gupta, V.K.; Moradi, O.; Makhlouf, A.S.H.; Sillanpää, M.; Nadagouda, M.N.; Sadegh, H.; Shahryari-ghoshekandi, R.; Pal, A.; Wang, Z.; et al. A comparative study on the basis of adsorption capacity between CNTs and activated carbon as adsorbents for removal of noxious synthetic dyes: A review. *J. Nanostruct. Chem.* **2015**, *5*, 227–236. [CrossRef]
262. Ghaedi, M.; Khajehsharifi, H.; Yadkuri, A.H.; Roosta, M.; Asghari, A. Oxidized multiwalled carbon nanotubes as efficient adsorbent for bromothymol blue. *Toxicol. Environ. Chem.* **2012**, *94*, 873–883. [CrossRef]
263. Mahmoodian, H.; Moradi, O.; Shariatzadeha, B.; Salehf, T.A.; Tyagi, I.; Maity, A.; Asif, M.; Gupta, V.K. Enhanced removal of methyl orange from aqueous solutions by poly HEMA–chitosan-MWCNT nano-composite. *J. Mol. Liq.* **2015**, *202*, 189–198. [CrossRef]
264. Duman, O.; Tunç, S.; Polat, T.G.; Bozoğlan, B.K. Synthesis of magnetic oxidized multiwalled carbon nanotube-κ-carrageenan-Fe 3 O 4 nanocomposite adsorbent and its application in cationic Methylene Blue dye adsorption. *Carbohydr. Polym.* **2016**, *147*, 79–88. [CrossRef]
265. Sadegh, H.; Zare, K.; Maazinejad, B.; Shahryari-ghoshekandi, R.; Tyagi, I.; Agarwal, S.; Gupta, V.K. Synthesis of MWCNT-COOH-Cysteamine composite and its application for dye removal. *J. Mol. Liq.* **2016**, *215*, 221–228. [CrossRef]
266. Wang, Y.; Huang, H.; Wei, X. Influence of wastewater precoagulation on adsorptive filtration of pharmaceutical and personal care products by carbon nanotube membranes. *Chem. Eng. J.* **2018**, *333*, 66–75. [CrossRef]
267. Wang, S.; Liang, S.; Liang, P.; Zhang, X.; Sun, J.; Wu, S.; Huang, X. In-situ combined dual-layer CNT/PVDF membrane for electrically-enhanced fouling resistance. *J. Memb. Sci.* **2015**, *491*, 37–44. [CrossRef]
268. Wang, Y.; Zhu, J.; Huang, H.; Cho, H.-H. Carbon nanotube composite membranes for microfiltration of pharmaceuticals and personal care products: Capabilities and potential mechanisms. *J. Memb. Sci.* **2015**, *479*, 165–174. [CrossRef]
269. Jahangiri-Rad, M.; Nadafi, K.; Mesdaghinia, A.; Nabizadeh, R.; Younesian, M.; Rafiee, M. Sequential study on reactive blue 29 dye removal from aqueous solution by peroxy acid and single wall carbon nanotubes: Experiment and theory. *Iran. J. Environ. Health Sci. Eng.* **2013**, *10*, 5. [CrossRef] [PubMed]
270. Engel, M.; Chefetz, B. Adsorption and desorption of dissolved organic matter by carbon nanotubes: Effects of solution chemistry. *Environ. Pollut.* **2016**, *213*, 90–98. [CrossRef]
271. Ajmani, G.S.; Goodwin, D.; Marsh, K.; Fairbrother, D.H.; Schwab, K.J.; Jacangelo, J.G.; Huang, H. Modification of low pressure membranes with carbon nanotube layers for fouling control. *Water Res.* **2012**, *46*, 5645–5654. [CrossRef] [PubMed]
272. Yang, X.; Lee, J.; Yuan, L.; Chae, S.-R.; Peterson, V.K.; Minett, A.I.; Yin, Y.; Harris, A.T. Removal of natural organic matter in water using functionalised carbon nanotube buckypaper. *Carbon N. Y.* **2013**, *59*, 160–166. [CrossRef]
273. Deng, J.; Shao, Y.; Gao, N.; Deng, Y.; Tan, C.; Zhou, S.; Hu, X. Multiwalled carbon nanotubes as adsorbents for removal of herbicide diuron from aqueous solution. *Chem. Eng. J.* **2012**, *193–194*, 339–347. [CrossRef]
274. Hamdi, H.; De La Torre-Roche, R.; Hawthorne, J.; White, J.C. Impact of non-functionalized and amino-functionalized multiwall carbon nanotubes on pesticide uptake by lettuce (*Lactuca sativa* L.). *Nanotoxicology* **2015**, *9*, 172–180. [CrossRef] [PubMed]
275. Rocha, J.-D.R.; Rogers, R.E.; Dichiara, A.B.; Capasse, R.C. Emerging investigators series: Highly effective adsorption of organic aromatic molecules from aqueous environments by electronically sorted single-walled carbon nanotubes. *Environ. Sci. Water Res. Technol.* **2017**, *3*, 203–212. [CrossRef]
276. Dichiara, A.B.; Harlander, S.F.; Rogers, R.E. Fixed bed adsorption of diquat dibromide from aqueous solution using carbon nanotubes. *RSC Adv.* **2015**, *5*, 61508–61512. [CrossRef]
277. Srivastava, A.; Srivastava, O.N.; Talapatra, S.; Vajtai, R.; Ajayan, P.M. Carbon nanotube filters. *Nat. Mater.* **2004**, *3*, 610–614. [CrossRef]
278. Tahaikt, M.; El Habbani, R.; Ait Haddou, A.; Achary, I.; Amor, Z.; Taky, M.; Alami, A.; Boughriba, A.; Hafsi, M.; Elmidaoui, A. Fluoride removal from groundwater by nanofiltration. *Desalination* **2007**, *212*, 46–53. [CrossRef]
279. Fornasiero, F.; Park, H.G.; Holt, J.K.; Stadermann, M.; Grigoropoulos, C.P.; Noy, A.; Bakajin, O. Ion exclusion by sub-2-nm carbon nanotube pores. *Proc. Natl. Acad. Sci. USA* **2008**, *105*, 17250–17255. [CrossRef]

280. Noy, A.; Park, H.G.; Fornasiero, F.; Holt, J.K.; Grigoropoulos, C.P.; Bakajin, O. Nanofluidics in carbon nanotubes. *Nano Today* **2007**, *2*, 22–29. [CrossRef]
281. Hummer, G.; Rasaiah, J.C.; Noworyta, J.P. Water conduction through the hydrophobic channel of a carbon nanotube. *Nature* **2001**, *414*, 188–190. [CrossRef] [PubMed]
282. Moradi, O. Adsorption Behavior of Basic Red 46 by Single-Walled Carbon Nanotubes Surfaces. *Fuller. Nanotub. Carbon Nanostructures* **2013**, *21*, 286–301. [CrossRef]
283. Yang, S.; Wang, L.; Zhang, X.; Yang, W.; Song, G. Enhanced adsorption of Congo red dye by functionalized carbon nanotube/mixed metal oxides nanocomposites derived from layered double hydroxide precursor. *Chem. Eng. J.* **2015**, *275*, 315–321. [CrossRef]
284. Konicki, W.; Pełech, I.; Mijowska, E.; Jasińska, I. Adsorption of anionic dye Direct Red 23 onto magnetic multi-walled carbon nanotubes-Fe3C nanocomposite: Kinetics, equilibrium and thermodynamics. *Chem. Eng. J.* **2012**, *210*, 87–95. [CrossRef]
285. Setareh Derakhshan, M.; Moradi, O. The study of thermodynamics and kinetics methyl orange and malachite green by SWCNTs, SWCNT-COOH and SWCNT-NH2 as adsorbents from aqueous solution. *J. Ind. Eng. Chem.* **2014**, *20*, 3186–3194. [CrossRef]
286. Zhao, D.; Zhang, W.; Chen, C.; Wang, X. Adsorption of Methyl Orange Dye Onto Multiwalled Carbon Nanotubes. *Procedia Environ. Sci.* **2013**, *18*, 890–895. [CrossRef]
287. Ahmad, A.; Razali, M.H.; Mamat, M.; Mehamod, F.S.B.; Anuar Mat Amin, K. Adsorption of methyl orange by synthesized and functionalized-CNTs with 3-aminopropyltriethoxysilane loaded TiO2 nanocomposites. *Chemosphere* **2017**, *168*, 474–482. [CrossRef]
288. Robati, D.; Mirza, B.; Ghazisaeidi, R.; Rajabi, M.; Moradi, O.; Tyagi, I.; Agarwal, S.; Gupta, V.K. Adsorption behavior of methylene blue dye on nanocomposite multi-walled carbon nanotube functionalized thiol (MWCNT-SH) as new adsorbent. *J. Mol. Liq.* **2016**, *216*, 830–835. [CrossRef]
289. Shih, M.-W.; Chin, C.-J.M.; Yu, Y.-L. The role of oxygen-containing groups on the adsorption of bisphenol-A on multi-walled carbon nanotube modified by HNO_3 and KOH. *Process Saf. Environ. Prot.* **2017**, *112*, 308–314. [CrossRef]
290. Kuo, C.-Y. Comparison with as-grown and microwave modified carbon nanotubes to removal aqueous bisphenol A. *Desalination* **2009**, *249*, 976–982. [CrossRef]
291. Liao, Q.; Sun, J.; Gao, L. Adsorption of chlorophenols by multi-walled carbon nanotubes treated with HNO_3 and NH_3. *Carbon N. Y.* **2008**, *46*, 553–555. [CrossRef]
292. Mubarak, N.M.; Sazila, N.; Nizamuddin, S.; Abdullah, E.C.; Sahu, J.N. Adsorptive removal of phenol from aqueous solution by using carbon nanotubes and magnetic biochar. *Nano World J.* **2017**, *3*, 32–37. [CrossRef]
293. Yao, Y.-X.; Li, H.-B.; Liu, J.-Y.; Tan, X.-L.; Yu, J.-G.; Peng, Z.-G. Removal and Adsorption of p-Nitrophenol from Aqueous Solutions Using Carbon Nanotubes and Their Composites. *J. Nanomater.* **2014**, *2014*, 1–9. [CrossRef]
294. Diaz-Flores, P.E.; López-Urías, F.; Terrones, M.; Rangel-Mendez, J.R. Simultaneous adsorption of Cd^{2+} and phenol on modified N-doped carbon nanotubes: Experimental and DFT studies. *J. Colloid Interface Sci.* **2009**, *334*, 124–131. [CrossRef]
295. Tóth, A.; Törőcsik, A.; Tombácz, E.; László, K. Competitive adsorption of phenol and 3-chlorophenol on purified MWCNTs. *J. Colloid Interface Sci.* **2012**, *387*, 244–249. [CrossRef]
296. Arasteh, R.; Masoumi, M.; Rashidi, A.M.; Moradi, L.; Samimi, V.; Mostafavi, S.T. Adsorption of 2-nitrophenol by multi-wall carbon nanotubes from aqueous solutions. *Appl. Surf. Sci.* **2010**, *256*, 4447–4455. [CrossRef]
297. Kassem, A.; Ayoub, G.M.; Malaeb, L. Antibacterial activity of chitosan nano-composites and carbon nanotubes: A review. *Sci. Total Environ.* **2019**, *668*, 566–576. [CrossRef]
298. Smith, S.C.; Rodrigues, D.F. Carbon-based nanomaterials for removal of chemical and biological contaminants from water: A review of mechanisms and applications. *Carbon N. Y.* **2015**, *91*, 122–143. [CrossRef]
299. Brady-Estévez, A.S.; Kang, S.; Elimelech, M. A Single-Walled-Carbon-Nanotube Filter for Removal of Viral and Bacterial Pathogens. *Small* **2008**, *4*, 481–484. [CrossRef]
300. Lu, C.; Su, F. Adsorption of natural organic matter by carbon nanotubes. *Sep. Purif. Technol.* **2007**, *58*, 113–121. [CrossRef]
301. Kang, S.; Pinault, M.; Pfefferle, L.D.; Elimelech, M. Single-Walled Carbon Nanotubes Exhibit Strong Antimicrobial Activity. *Langmuir* **2007**, *23*, 8670–8673. [CrossRef]
302. Ihsanullah; Asmaly, H.A.; Saleh, T.A.; Laoui, T.; Gupta, V.K.; Atieh, M.A. Enhanced adsorption of phenols from liquids by aluminum oxide/carbon nanotubes: Comprehensive study from synthesis to surface properties. *J. Mol. Liq.* **2015**, *206*, 176–182. [CrossRef]
303. Bohonak, D.; Zydney, A. Compaction and permeability effects with virus filtration membranes. *J. Memb. Sci.* **2005**, *254*, 71–79. [CrossRef]
304. Mostafavi, S.T.; Mehrnia, M.R.; Rashidi, A.M. Preparation of nanofilter from carbon nanotubes for application in virus removal from water. *Desalination* **2009**, *238*, 271–280. [CrossRef]
305. Savage, N.; Diallo, M.S. Nanomaterials and Water Purification: Opportunities and Challenges. *J. Nanopart. Res.* **2005**, *7*, 331–342. [CrossRef]
306. Li, Q.; Mahendra, S.; Lyon, D.Y.; Brunet, L.; Liga, M.V.; Li, D.; Alvarez, P.J.J. Antimicrobial nanomaterials for water disinfection and microbial control: Potential applications and implications. *Water Res.* **2008**, *42*, 4591–4602. [CrossRef]
307. Nepal, D.; Balasubramanian, S.; Simonian, A.L.; Davis, V.A. Strong Antimicrobial Coatings: Single-Walled Carbon Nanotubes Armored with Biopolymers. *Nano Lett.* **2008**, *8*, 1896–1901. [CrossRef]

308. Cortes, P.; Deng, S.; Smith, G.B. The Adsorption Properties of Bacillus atrophaeus Spores on Single-Wall Carbon Nanotubes. *J. Sens.* **2009**, *2009*, 1–6. [CrossRef]
309. Ong, Y.T.; Ahmad, A.L.; Zein, S.H.S.; Tan, S.H. A review on carbon nanotubes in an environmental protection and green engineering perspective. *Braz. J. Chem. Eng.* **2010**, *27*, 227–242. [CrossRef]
310. Yuan, W.; Jiang, G.; Che, J.; Qi, X.; Xu, R.; Chang, M.W.; Chen, Y.; Lim, S.Y.; Dai, J.; Chan-Park, M.B. Deposition of Silver Nanoparticles on Multiwalled Carbon Nanotubes Grafted with Hyperbranched Poly(amidoamine) and Their Antimicrobial Effects. *J. Phys. Chem. C* **2008**, *112*, 18754–18759. [CrossRef]
311. Morones, J.R.; Elechiguerra, J.L.; Camacho, A.; Holt, K.; Kouri, J.B.; Ramírez, J.T.; Yacaman, M.J. The bactericidal effect of silver nanoparticles. *Nanotechnology* **2005**, *16*, 2346–2353. [CrossRef]
312. Ihsanullah; Laoui, T.; Al-Amer, A.M.; Khalil, A.B.; Abbas, A.; Khraisheh, M.; Atieh, M.A. Novel anti-microbial membrane for desalination pretreatment: A silver nanoparticle-doped carbon nanotube membrane. *Desalination* **2015**, *376*, 82–93. [CrossRef]
313. Nie, C.; Yang, Y.; Cheng, C.; Ma, L.; Deng, J.; Wang, L.; Zhao, C. Bioinspired and biocompatible carbon nanotube-Ag nanohybrid coatings for robust antibacterial applications. *Acta Biomater.* **2017**, *51*, 479–494. [CrossRef]
314. Morsi, R.E.; Alsabagh, A.M.; Nasr, S.A.; Zaki, M.M. Multifunctional nanocomposites of chitosan, silver nanoparticles, copper nanoparticles and carbon nanotubes for water treatment: Antimicrobial characteristics. *Int. J. Biol. Macromol.* **2017**, *97*, 264–269. [CrossRef]
315. Chi, M.-F.; Wu, W.-L.; Du, Y.; Chin, C.-J.M.; Lin, C.-C. Inactivation of Escherichia coli planktonic cells by multi-walled carbon nanotubes in suspensions: Effect of surface functionalization coupled with medium nutrition level. *J. Hazard. Mater.* **2016**, *318*, 507–514. [CrossRef]
316. Al-Hakami, S.M.; Khalil, A.B.; Laoui, T.; Atieh, M.A. Fast Disinfection of Escherichia coli Bacteria Using Carbon Nanotubes Interaction with Microwave Radiation. *Bioinorg. Chem. Appl.* **2013**, *2013*, 1–9. [CrossRef]